AN ABSTRACT OF THE THESIS OF

K. Todd Holland for the degree of Master of Science in

Oceanography presented on March 31, 1992.

Title: The Statistical Distribution of Swash Maxima on Natural Beaches

Abstract approved: Robert A. Holman

Beach response to overwash processes is a topic of significant importance. Two particular aspects of this topic were chosen for detailed analysis: the distribution of maximum wave runup elevations and the cross-beach celerity gradient of overwash bores on natural beaches. Data were collected using both traditional nearshore instrumentation and recently developed video-based techniques.

Field data from three separate experiments suggest that swash elevations may be regarded as a stochastic process whose maxima have a specific probability distribution function. The exact form of the maxima distribution depends solely on the relative bandwidth of the swash power spectrum and the root-mean-square value of the swash time series. Numerical simulations indicate that the linear assumptions required by the distribution model are commonly violated. Nevertheless, the qualitative trends suggested by the model are applicable to the probability statistics for all of the data.

Overwash celerity data were collected at a site on the Isles Dernieres, LA barrier island chain during Hurricane Gilbert in September 1988. A video technique was applied that

allowed the quantification of overwash bore celerity vectors along several cross-shore transects. Maximum celerities were found to exceed 2 m/sec. The cross-beach velocity structure can be characterized generally as having a maximum celerity at the berm crest with a linear decrease in velocity across the washover flat. Using the celerity results, a simple model of cross-beach overwash sediment transport is discussed.

Results from both investigations demonstrate that important attributes of runup and overwash processes can be sufficiently sampled using video techniques. More work is needed in terms of understanding the influence of overwash processes, specifically in the areas of runup trajectory and celerity characteristics, the interaction between fluid flow and bed permeability, and the regional scale forcing of sea level elevation.

The Statistical Distribution of Swash Maxima on Natural Beaches

by

K. Todd Holland

A THESIS

submitted to

Oregon State University

in partial fulfillment of
the requirements for the
degree of

Master of Science

Completed March 31, 1992

Commencement June 1992

APPROVED:

Redacted for Privacy

Professor of Oceanography in charge of major

Redacted for Privacy

Dean of the College of Oceanography

Redacted for Privacy

Dean of Graduate School

Date thesis is presented March 31, 1992

Typed by Todd Holland for Todd Holland

ACKNOWLEDGEMENTS

I arrived at Oregon State on August 21, 1989 with direction. My employers at the USGS had provided me with a unique data set that cried out for interpretation. They also provided the funds for me to do the analysis (Thanks Ab). I had the motivation for why this study was important, enough data to fill the largest available hard disk at that time (200 MB), and a robust set of tools to do the analysis. Cindy and I will be out of here in no time, I thought. Little did I realize that I would become the Coastal group's record holder for the longest period of time taken to complete a Master's degree.

To be fair, let me clarify the problem. I was a geologist, Rob wasn't. Although I thought adjectives and adverbs were well suited to describing nature, Rob explained that nature preferred mathematical relationships and Greek symbols. This became clear to me after probably one of the best presentations by a student I had ever seen. The topic concerned the Mecca of all civilization (Flathead Lake) and the speaker was Mark Lorang. This young scientist discussed some amazing results from an experiment he had single-handedly put together with little or no funding. Then the questions from the scientists came. "Did you depth correct the pressure sensors?" "What quantitative models do you have for sediment transport?" "Is there evidence for leaky modes or edge waves?" Blah, blah, blah, they went on for what seemed like hours. I was crushed to realize that rather than being directed, I was misdirected and unprepared.

What made my eventually successful attempt to become the new record holder rewarding was that it required getting help from others. I would like to thank the Coastal group "scientists", Rob Holman, Paul Komar, Reggie Beach, Mike Freilich, ex-officio member Joan Oltman-Shay and honorary member Tony Bowen for showing me the equations and helping me pronounce the symbols. Others contributed on the numerical

side including: Bob Guza, Dudley Chelton, Chuck Sollitt, Bob Hudspeth and Peter Bottomley. This work would not have been possible without the advice and distractions provided by Tom, Mark and Pete and the encouragement from Christine, Lynn, Terri, Mary Lynn, Dave, Jim T. and John M. Technical support at OSU was provided by John Stanley, Marcia Turnbull, Chuck Sears, Mark Johnson and Tom Leach while long distance support was provided by Terry Kelley, John Dingler, Tom Reiss, Rob Wertz, Rob Holder and the crew at the FRF. Thanks again to Abby and Rob for getting me started and redirecting me in my endeavors. I would also like to remember Paul O'Neill not only for being one of the most interesting and helpful people I have ever met, but also for being a true friend.

Not to forget my beginnings, I sincerely appreciate the support and caring given to me by my family: Mom, Dad, Stan, Debra, Tommy, Andy and Pam. Thanks most of all to the other two members of my cord of three strands, Cindy and the Lord, for I never could have made it without your being with me.

TABLE OF CONTENTS

LIST OF FIGURES

LIST OF TABLES

THE STATISTICAL DISTRIBUTION OF SWASH MAXIMA ON NATURAL BEACHES

CHAPTER ONE: GENERAL INTRODUCTION

Scientific studies of the effects of storms and hurricanes on barrier island topography have emphasized dramatic shoreline changes that have been loosely categorized as beach erosion. In many instances, however, observed erosion in one area is often partially compensated for by deposition in another area. The beach process of overwash is effective in transporting sediment between the locations of deposition and erosion. Overwash occurs during extreme storm events that force water over the top of the most landward berm or dune line. This overwash surge may contain sediment eroded by waves or may entrain sediment as it travels across the barrier flat. As the flow subsides, the surge velocity decreases and sediment falls out of suspension, thereby increasing the elevation of the beach or barrier island. In this manner, overwash provides a mechanism for maintaining the physical integrity of barriers and has long been recognized as an important parameter in the overall sediment budget of barrier islands. Yet the dynamics of overwash processes are poorly understood. Given its geological importance to barrier islands and its application to engineering considerations such as seawall overtopping, dune construction and shoreline setback criteria, a more thorough understanding of overwash dynamics is needed.

Most previous attempts to explain overwash occurrence in terms of meteorologic and oceanographic forcing parameters have been primarily qualitative, consisting of descriptions of the importance of overwash to the overall sediment budget of barrier islands and of the climatic and sea surface conditions during overwash. However, it is

possible to quantitatively describe overwash processes. Overwash results from the forcing of nearshore water surface elevations above the maximum berm or dune height. Therefore the summation of the magnitudes of the various collinear forces represents the highest attainable sea level elevation. Numerous regional factors exist that can cause elevation of coastal sea level including gravitational and radiational tides, geostrophic currents, river discharge, and storm surge. Additional sea surface elevation results from localized effects expressed as wave runup. Although generally considered a beachface process, wave runup is closely related to overwash in that overwash results from the overtopping of the berm by the highest runups. As such, overwash flow characteristics have memory and are strongly dependent upon the flow characteristics of the preceding runup.

Even though the forcing concept is relatively simple, prediction of the likelihood of overwash at a given location is complicated and depends upon our ability to resolve the respective magnitudes of each of the forces involved. Furthermore, quantification of the amounts of beach change resulting from a particular overwash event is strongly dependent upon not only the magnitudes of each of the forcing parameters, but also upon the characteristics of their interaction. As a starting point on this complicated subject, we chose to investigate an important local forcing function in overwash occurrence, namely wave runup, and also to attempt a first order parameterization of overwash sediment transport.

This thesis has two primary objectives, both of which relate to the beach response to overwash processes. The first is to characterize the form of the probability density function of runup maxima. Such a characterization is necessary for accurate prediction of overwash occurrence in that the form of the function gives the magnitude of the local forcing. The second objective is to develop a simple model of overwash sediment

transport using observations of overwash celerities. An understanding of overwash sediment transport is crucial to estimations of beach change resulting from overwash events. Fulfillment of both objectives required the development of data acquisition and analysis techniques using video recordings. These techniques are applicable to overwash, as well as other nearshore processes.

Chapter Two, titled "The Statistical Distribution of Swash Maxima on Natural Beaches" will be submitted to the *J. Geophys. Res.* with co-author Dr. Rob Holman. In this chapter, we present a statistical theory that describes the distribution of maxima of any stochastic process. Although runup is not generally considered as a linear, Gaussian process, certain observations of quasi-linearity in the runup field data compelled us to attempt to describe the probability distribution of swash maxima using the statistical theory. We determine that although there are often significant discrepancies between the theory and observations, the qualitative trends of the theory are appropriate.

In Chapter Three, "Estimation of Overwash Bore Velocities Using Video Techniques", a video technique is used to quantify the cross-beach gradients in overwash bore velocities. This work has been published in the *Proceedings of Coastal Sediments '91* (Holland et al., 1991). The findings show a monotonic decrease in overwash celerity with increasing distance from the berm. Maximum celerities were shown to be much larger than predicted using shallow water wave or bore theories. The observations emphasize the importance of initial velocity conditions *seaward* of the berm, in other words, wave runup. This work is co-authored by Dr. Holman and Dr. Abby Sallenger. Dr. Holman aided in the determination of the relevant physics, while Dr. Sallenger advocated the need for a sediment transport model.

CHAPTER TWO:

THE STATISTICAL DISTRIBUTION OF SWASH MAXIMA ON NATURAL BEACHES

Abstract

Field data from three experiments are presented which suggest that swash elevations may be regarded as a stochastic process whose maxima have a specific probability distribution function. The exact form of the maxima distribution depends solely on the relative bandwidth of the swash power spectrum and the root-mean-square value of the swash time series. Numerical simulations indicate that the linear assumptions required by the distribution model are commonly violated. Nevertheless, the qualitative trends suggested by the model are applicable to the probability statistics for all of the data.

Introduction

Estimation of extreme values of wave runup (shoreline water level) is of interest to oceanographers, ocean engineers and coastal planners. Many applications require accurate predictions of maximum runup elevations to allow choice of appropriate and economically feasible design heights for shore protection structures such as seawalls. Furthermore, the ability to predict maximum runup elevations is needed in the modeling of beach response to various wave energy regimes. In the following we present a statistical model that estimates the distribution of runup maxima under the assumption that runup can be approximated as a linear, Gaussian process.

Figure II.1 diagrams a hypothetical runup time series. For a given set of wave conditions, the runup elevation $\eta(t)$ can be decomposed into two components. The setup, $\bar{\eta}$, is taken to be the mean water surface elevation above the still water level, while swash, $\eta'(t)$, is defined as fluctuations of the runup about the setup level, $\eta'(t) = \eta(t) - \bar{\eta}$. Laboratory researchers commonly use the term runup to describe discrete maximum elevations rather than a continuous process, and make no distinction between setup and swash. We would like to remove this ambiguity by defining swash maxima ζ to be the difference in elevation between any local crest in $\eta(t)$ and the setup level. Although this definition of local maxima is less common than the zero-crossing definition, R, used by other researchers, the distribution of local maxima can be derived theoretically. One major difference between the two maxima definitions is that for non-narrow-band processes, the local maxima definition can be either positive or negative; while the zero-crossing definition allows for only positive maxima. Further use of the above symbols will pertain to normalized variables, whereas reference to dimensional forms will be indicated by a caret, ^.

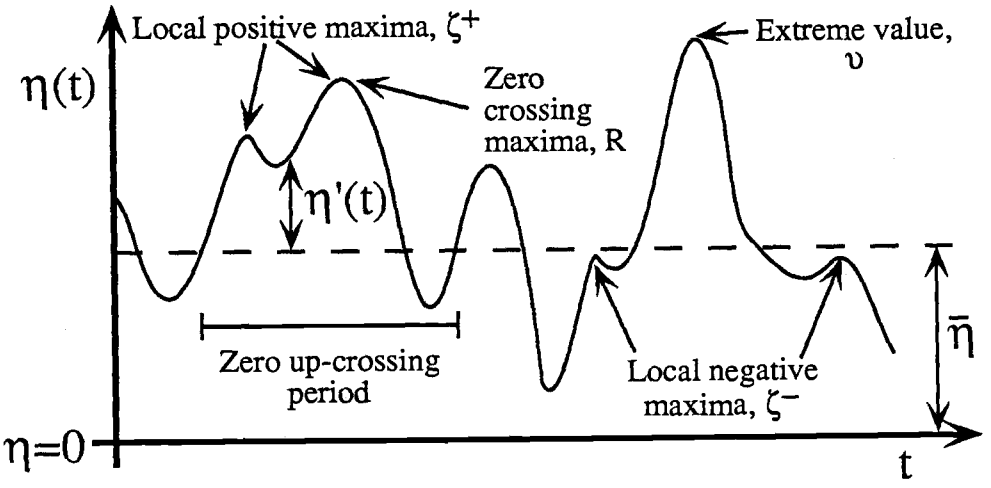

Figure II.1. Definition diagram of runup variables.

Theories describing the swash motions of irregular, breaking waves (review by LeMehaute et al., 1968) are difficult to apply to field and laboratory data. However, several empirical methods for determining the distribution of irregular wave runup maxima have been formulated. One of the earliest methods, given by Saville (1962), relies on individual wave analysis to construct the runup maxima distribution. Basically, a runup relation developed under monochromatic wave conditions is applied to individuals from an irregular wave train. The assumption inherent to this method is known as the hypothesis of equivalency. Equivalency is not an assumption of linearity in terms of direct superposition. Rather, the hypothesis presumes linear relationships between statistical averages only, not individuals. The resulting empirical distribution is calculated graphically for each particular combination of wave steepness and structure slope assuming independence of offshore wave height and length.

Battjes (1971) extended Saville's method to include conditions of varying correlation between wavelength and wave height by making the additional assumption that the maximum monochromatic runup elevation, $\hat{R}$, is given by Hunt's (1959) empirical equation for waves breaking on a smooth slope:

$$\hat{R} = C\sqrt{\hat{H}_o \hat{L}_o}\tan\beta \qquad \text{(II.1)}$$

where $\hat{H}_o$ is the offshore wave height; $\hat{L}_o$ is the offshore wavelength; tan β is the beach slope and C is an empirical constant. Using a derivation based on equivalency and Equation (II.1), the distribution of non-dimensional runup maxima of breaking waves on constant slopes, $R = \dfrac{\hat{R}}{\sqrt{\hat{H}_o \hat{L}_o}\tan\beta}$, is then given by:

$$p(R) = \frac{\pi^2}{2}\frac{R^3}{1-k^2} I_0\left(\frac{\pi}{2}\frac{k}{1-k^2}\right) R^2 K_0\left(\frac{\pi}{2}\frac{R^2}{1-k^2}\right) \qquad \text{(II.2)}$$

where k^2 is the coefficient of linear correlation between H_0^2 and L_0^2, and where the functions I_0 and K_0 are the zero order modified Bessel functions of the first and third kinds. Figure II.2 is a graph of Equation (II.2) for six values of k from 0 to 1. For the limiting case of linear dependence of normalized wave height and length (k=1), asymptotic expansion of the Bessel functions yields the one-dimensional Rayleigh distribution. Battjes mentions that the above equation compares well with Saville's data (k=0) except on steep slopes where few waves break, making Hunt's equation inapplicable.

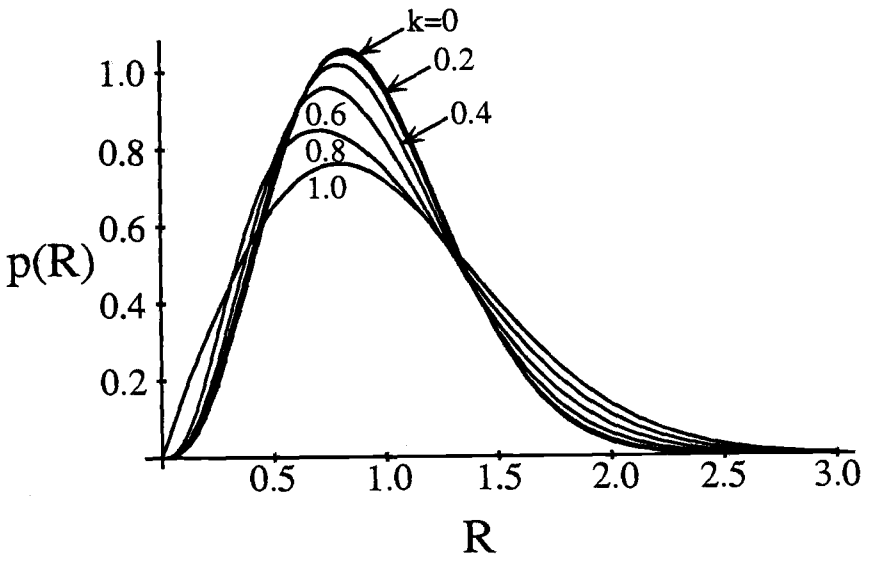

Figure II.2. Probability density of normalized runup maxima for various values of the correlation parameter k (from Battjes, 1971).

The hypothesis of equivalency used in the linear methods described above is inconsistent for conditions of significant infragravity energy, commonly a dominant component of field runup signals (Holman, 1981), for which there is no equivalent offshore wave. Although other theoretical runup distribution models have been proposed (Ahrens 1978, 1983; Nielsen and Hanslow 1991; Sawaragi and Iwata 1984) they either depend upon equivalency or rely upon empirical "weighting" coefficients that obscure the physics of their development. Furthermore, most of the previous models have been largely unconstrained by field data.

Our principle objective is to characterize the wave runup maxima probability density function (pdf) for field data in terms of a model that does not assume equivalency, but still has a physical basis. In the following we will describe a probabilistic model for the maxima of an arbitrary Gaussian process in which the form of the pdf depends solely on parameters derived from the process spectrum. The model is then applied to data from three separate field sites taken under a variety of environmental conditions. This application involves the use of numerical simulations to assess the validity of the assumptions required by the model, namely linearity. Finally, the implications of deviation from these assumptions are discussed.

Statistical Model Application

Following Rice (1944, 1945), Cartwright and Longuet-Higgins (1956), hereafter referred to as CLH56, present the theoretical, statistical distribution of maxima of an arbitrary stochastic function, f(t), formed as the sum of an infinite number of sine waves of random phase:

$$f(t) = \sum_{n}^{\infty} c_n \cos(\sigma_n t + \phi_n) \tag{II.3}$$

where the frequencies, σ_n, are distributed densely in the interval $(0,\infty)$, the phases, ϕ_n, are uniformly distributed between 0 and 2π; and the amplitudes, c_n, are given by the energy spectrum. Through application of the central limit theorem, f(t) can be shown to be a Gaussian process with a pdf given by the Gaussian (or standard normal) distribution. Although not all Gaussian processes are necessarily linear, it is common to approximate linear processes as being given by Equation (II.3). Under this assumption, the terms linear and Gaussian can be used interchangeably.

The pdf of the normalized maxima, $\zeta = \hat{\zeta}/\sqrt{m_0}$ of f(t) is given by:

$$p(\zeta) = \frac{1}{\sqrt{2\pi}}\left[\varepsilon e^{-\frac{1}{2}\zeta^2/\varepsilon^2} + \sqrt{1-\varepsilon^2}\,\zeta e^{-\frac{1}{2}\zeta^2}\int_{-\infty}^{\zeta\sqrt{1-\varepsilon^2}/\varepsilon} e^{-\frac{1}{2}x^2}\,dx\right] \tag{II.4}$$

Thus the distribution of maxima will depend on only two parameters: a normalization factor, $\sqrt{m_0}$, which is the root mean square of f(t) and the spectral width parameter, ε, which represents the relative width of the energy density spectrum, $E(\sigma)$, of f(t):

$$\varepsilon^2 = \frac{m_0 m_4 - m_2^2}{m_0 m_4}; \qquad \text{where } m_n = \int_0^\infty E(\sigma)\sigma^n d\sigma \qquad \text{(II.5)}$$

Figure II.3 shows the range of maxima distributions as a function of the bandwidth parameter ε. For an infinitely narrow spectrum ($\varepsilon \to 0$), the distribution of ζ tends to a Rayleigh distribution:

$$p(\zeta) = \left\{ \begin{array}{ll} \zeta e^{-\frac{1}{2}\zeta^2} & (\zeta \geq 0) \\ 0 & (\zeta < 0) \end{array} \right\} \qquad \text{(II.6)}$$

As ε approaches its maximum value of 1, the distribution of ζ tends to a Gaussian distribution with standard deviation equal to 1 and zero mean

$$p(\zeta) = \frac{1}{\sqrt{2\pi}} e^{-\frac{1}{2}\zeta^2} \qquad \text{(II.7)}$$

Note that as the spectral width increases, the proportion of negative maxima increases, the mode of $p(\zeta)$ gradually decreases, the variance increases and the skewness decreases.

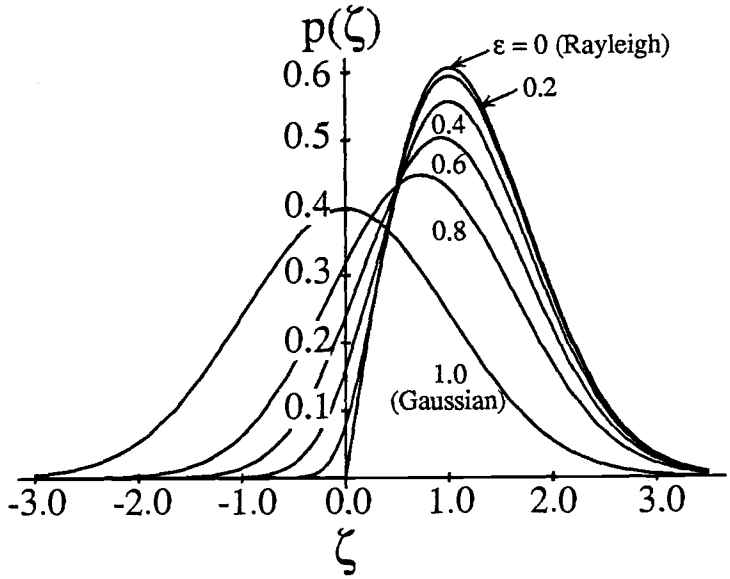

Figure II.3. Statistical distribution of maxima of a random process as a function of the spectral width parameter, ε (from Cartwright and Longuet-Higgins, 1956).

In addition to presenting a theoretical form of the distribution of maxima, the Cartwright and Longuet-Higgins model can be extended to predictions of specific extreme value parameters. We have presented the probability density function for maxima, ζ, of a random process in Equation (II.4). Our present goal is to present the distribution of the largest maximum, υ, that will occur in n maxima observations (see Figure II.1). The extreme maximum has a probability density function quite different from $p(\zeta)$, although they are derived similarly.

Ochi (1973) presents formulas for the prediction of extreme values of a random process given its spectral characteristics. He finds that extreme values from random variables are distributed according to the probability density function:

$$g(\upsilon) = [nf(\zeta)\{F(\zeta)\}^{n-1}]_{\zeta=\upsilon} \tag{II.8}$$

where $f(\upsilon)$ is the nondimensionalized probability density function given in Equation (II.4) reformulated to describe only positive maxima ($\zeta \geq 0$). $F(\upsilon)$ is the cumulative distribution function of $f(\upsilon)$. The "most probable extreme value", $\bar{\upsilon}$, is the modal value of $g(\upsilon)$ found as the solution of the derivative of Equation (II.8) with respect to υ

$$\frac{d}{d\upsilon}g(\upsilon) = f'(\upsilon)F(\upsilon) + (n-1)[f(\upsilon)]^2 = 0 \tag{II.9}$$

Solutions to Equation (II.9) can be found iteratively using Newton's method.

Most probable extremes, $\bar{\upsilon}$, are shown in Figure II.4 as a function of spectral width for ε values between 0 and 1. As seen in the figure, the effect of ε on the most probable extreme is most noticeable for ε greater than 0.9.

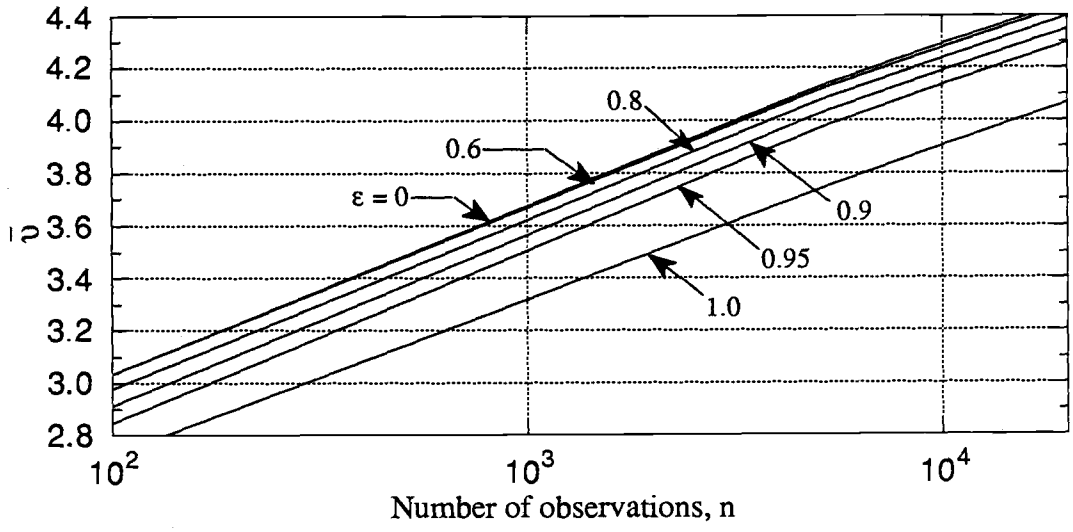

Figure II.4. Most probable extreme value, $\bar{\upsilon}$, as a function of ε (from Ochi, 1973).

There is a sizable probability, however, that $\bar{\upsilon}$ will be exceeded by the observed extreme value. Therefore, we desire to predict an extreme value for which the probability of exceedence is very small. Ochi (1973) derives the following relationship between the given probability of being exceeded, α, and the desired extreme value, υ_α, of the maxima of a random process having a spectral width value, ε:

$$\sqrt{1-\varepsilon^2}\,e^{-\frac{\upsilon_\alpha}{2}}\left\{1-\Phi\left(-\frac{\sqrt{1-\varepsilon^2}}{\varepsilon}\upsilon_\alpha\right)\right\}+\left\{1-\Phi\left(\frac{\upsilon_\alpha}{\varepsilon}\right)\right\}=\left(\frac{1+\sqrt{1-\varepsilon^2}}{2}\right)\left(\frac{\alpha}{n}\right) \qquad \text{(II.10)}$$

where the function $\Phi(u)$ in the above represents a form of the error function integral in Equation (II.4):

$$\Phi(u)=\frac{1}{\sqrt{2\pi}}\int_{-\infty}^{u} e^{-u^2/2}du \qquad \text{(II.11)}$$

Extreme values, υ_α, for a spectral width value of 0.9 are shown in Figure II.5 as a function of α.

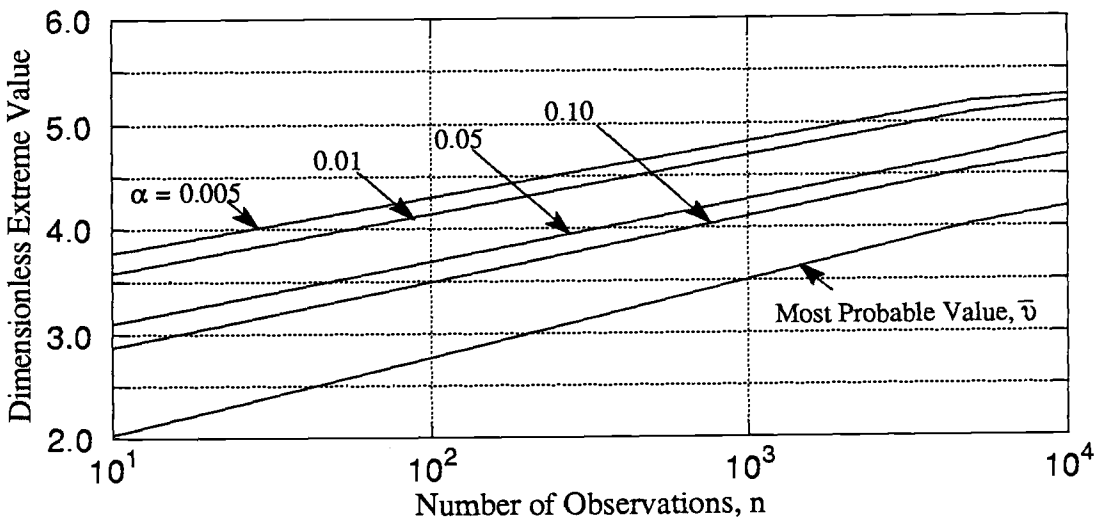

Figure II.5. Extreme values, υ_α, and $\bar{\upsilon}$, as a function of probability of being exceeded, α, for $\varepsilon = 0.9$ (after Ochi, 1973).

It may be somewhat surprising that we are attempting to describe swash motions using a linear model given the strong nonlinearities that are common in the nearshore zone. However, linear models have had considerable success in describing swash dynamics (Miche, 1951; Suhayda, 1974). In fact, the nonlinear, finite amplitude development of Carrier and Greenspan (1958) shows that under certain conditions the amplitude of the swash motion does not differ significantly from that given by linear theory. Additionally, wave kinematics (Guza and Thornton, 1980) and phase velocity (Thornton and Guza, 1982) observations have been shown to be consistent with linear theory in a region well beyond its theoretically applicable range. Therefore, extension of linear based hypotheses to describe swash maxima deserves consideration.

Field Measurements

The model was tested over a range of model parameters using results from three experiments: the Louisiana Barrier Island Erosion Study (Sallenger et al. 1987), the USWASH experiment and the DELILAH (Birkemeier et al., 1992) experiment. To our knowledge this work incorporates one of the largest and most accurate field runup data sets ever collected.

The Louisiana Barrier Island Erosion Study (LBIES) experiment took place on the barrier island of Isles Dernieres, LA and attempted to track the propagation of runup and overwash bores over low-lying topography. In this experiment, a resistance wire runup sensor provided runup data between Feb. 14-25, 1989. The USWASH experiment was conducted over a three day period at Scripps Beach in La Jolla, CA during June 1989. The objective of this experiment was to accurately sample swash processes using various methods. Both video-based and resistance wire runup sensors were deployed. However, only the video results will be presented in the model application. DELILAH was a multi-investigator study of nearshore dynamics on a barred beach, including the response of sand bars to waves. The experiment was located at the US Army Corps of Engineers Field Research Facility in Duck, NC. Over a three week period in October 1990, swash zone video recordings were made almost continuously during daylight hours.

The video recordings from USWASH and DELILAH were analyzed using a modified version of the "timestack" method described by Aagard and Holm (1989). Measured, shore-normal, beach transects, extending from the dry beach across the swash region were mapped onto the video image using known geometric transformations (Lippmann and Holman, 1989). Using an image processing system, pixel intensities along the entire transect were digitized and then written horizontally across a frame buffer. Subsequent

samples were "stacked" down the frame buffer such that cross-shore distance is represented along the horizontal axis and time increases down the screen. In this manner, timestacks provide visual information of the cross-shore variability of pixel intensity over time.

A typical timestack is shown in Figure II.6. Swash locations can be clearly identified by the sharp change in intensity between the darker beach surface and the lighter "foamy" edge of the swash bore. An appropriate inverse transformation to ground coordinates provides swash elevation measurement. The process is accomplished using standard image processing edge detection algorithms along with manual refinements. The vertical resolution of this technique for these experiments is typically O(1 cm).

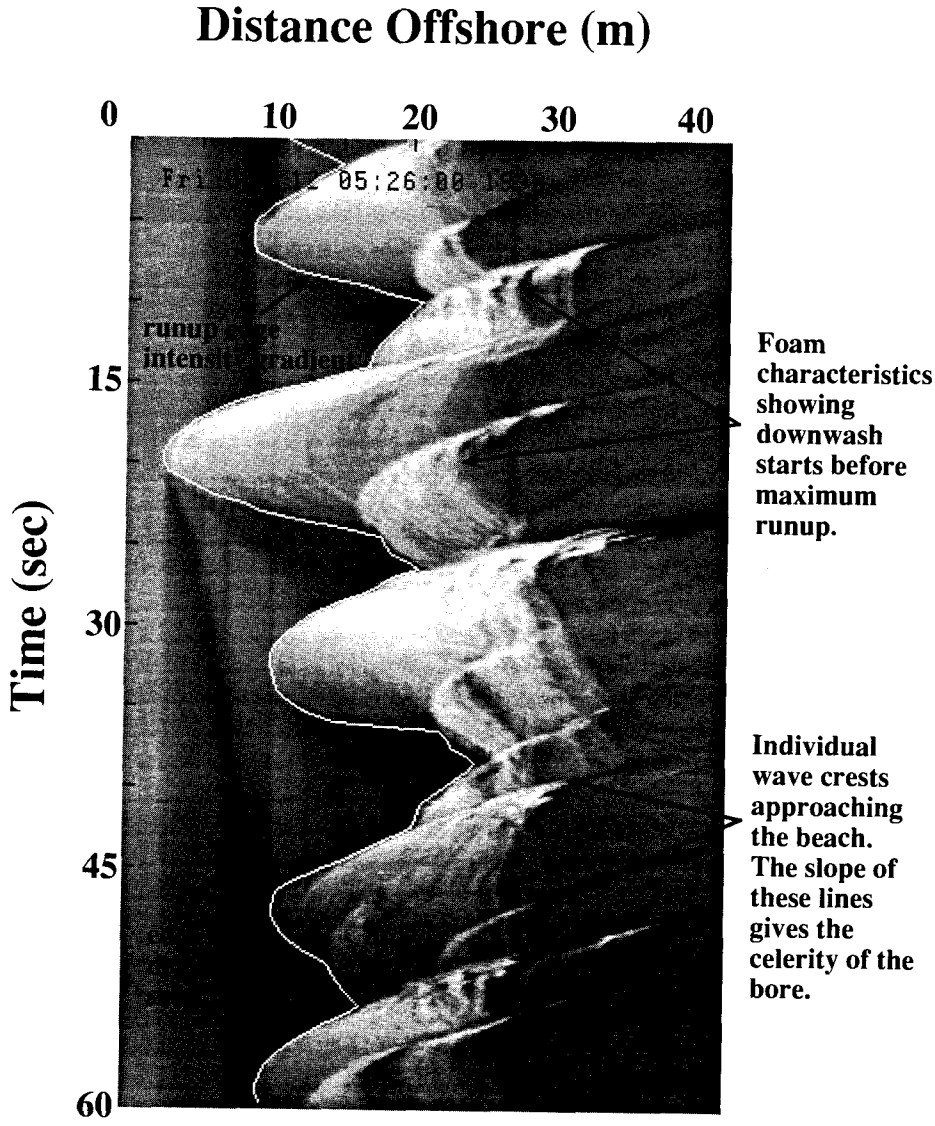

Figure II.6. "Timestack" from the DELILAH experiment showing the runup edge and swash characteristics.

The runup sensor measurements made during the LBIES utilized a dual wire resistance gauge (described by Guza and Thornton, 1982) deployed horizontally across the beach at a height, δ, above the sand surface. Accuracies and resolutions of this method as compared to the video measurements have been discussed previously (Holman and Guza, 1984) and are not extended here. However, it is noted that comparisons between the two methods (Holland and Holman, 1991) suggest that as $\delta \rightarrow 0$ the wire measurements approach the video results. For the present δ = 4 cm deployment, any significant discrepancies between methods are expected to be apparent only with regard to mean and variance values and not with regard to the distribution shapes.

The environmental conditions and beach types varied substantially among the three experiment locations (Table II.1). The data cover conditions ranging from incident (typical period O(10) seconds) to infragravity (period 20-300 seconds) energy dominated conditions, representing a variety of combinations of sea and swell. Offshore significant wave heights varied from 0.54 to 2.71 m, with peak periods between 5 and 13 s. Profile slopes ranged between 1:20 and approximately 1:10.

Table II.1. Ranges of environmental conditions at the different experiment locations.

Experiment	Dates	Location	Method	Hs [m]	T [s]	tan β
LBIES	2/14 - 2/25/89	Isles Dernieres, LA	Wire	0.58-0.87	4.0-6.0	0.05
USWASH	6/26 - 6/29/89	La Jolla, CA	Video	0.54-2.35	5.8-13.6	0.05
DELILAH	10/03 - 10/19/90	Duck, NC	Video	0.94-2.71	5.1-10.2	0.07

Data were selected for analysis based on an assessment of the performance of the timestack and runup wire methods described above. Those video records for which there was very low intensity contrast between beach and the swash (and therefore a larger probability of estimation error) were excluded. Similarly, wire data runs were also excluded whenever the sensor was fouled by debris. Data were also subjected to a run test

to verify stationarity (Bendat and Piersol, 1986). Runs showing trends in $\sqrt{m_0}$ inconsistent with random fluctuations were excluded from the analysis.

Ultimately, 85 time series were selected. In each case, the data were sampled at 2 Hz, with a record length of 2 hours giving a total of 14,336 data points. All data were quadratically detrended to remove any tidal fluctuations and the wave-induced setup. In addition, a low pass filter was applied to eliminate signals having periods shorter than 3 seconds. Spectral parameters required in the model were determined from smoothed versions of the measured spectra calculated with 112 degrees of freedom. Maxima were defined as having a zero first derivative and a second derivative value less than zero.

Results

Simulations

In order to verify the applicability and validity of the CLH56 model, synthetic time series were constructed by inverse Fourier transforming the observed spectrum, but with randomly selected Fourier phases, ϕ_n. This operation produces a simulated time series given by Equation (II.3) with identical model input parameters to the original time series. 1000 independent, realizations were produced for each observed swash time series, with appropriate statistics being computed in an identical manner to the field data.

The resulting simulations indicate no significant difference between the CLH56 model expectations and the synthetic maxima distributions. For each swash spectrum analyzed, the theoretical maxima pdf was within 1 standard deviation of the simulation results (see Figure II.7). This correspondence indicates that the CLH56 model is applicable for the particular spectral shapes common to the measured swash time series presented in this study. Therefore, any significant discrepancy between field observations and the model is highly suggestive of a nonlinear nature of the runup process.

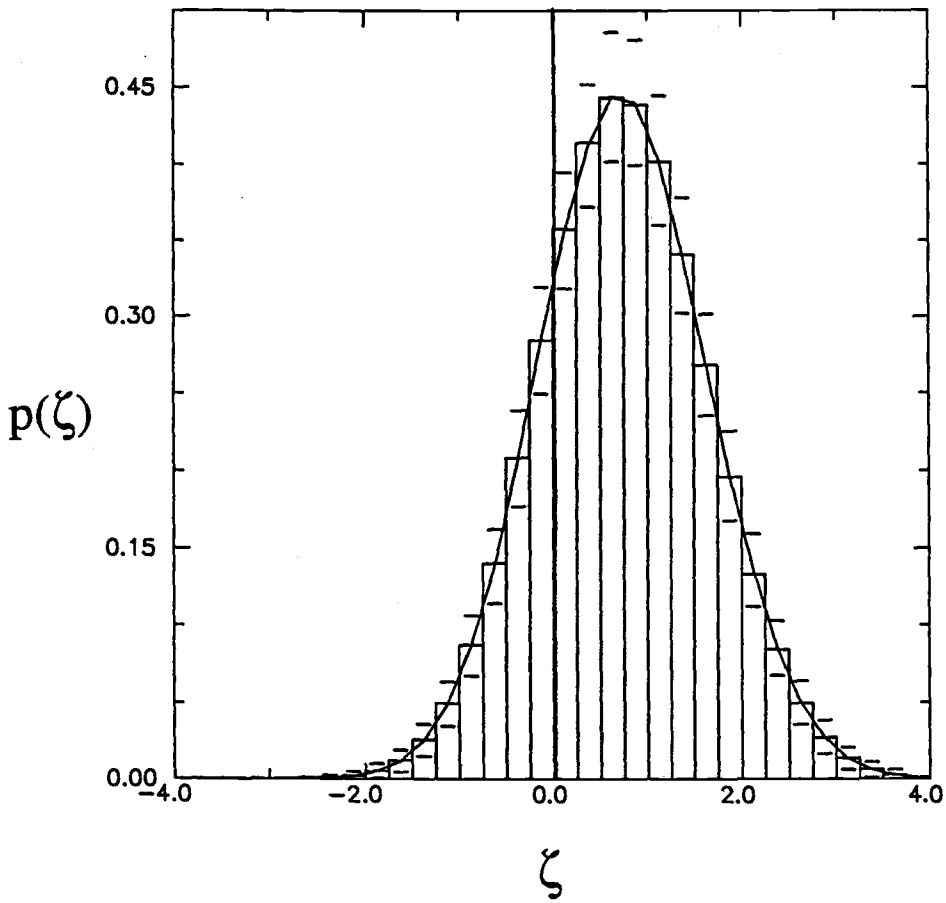

Figure II.7. Average of maxima pdfs using simulations compared to the theoretical pdf. The field data from the DELILAH experiment used to prepare the synthetic data has a spectral width value, $\varepsilon = 0.81$. 1 standard deviation error bars are indicated.

Linearity of Field Observations

The swash elevation time series were tested for Gaussianity (and hence the appropriateness of the linear superposition approximation) through the application of chi-square and Kolmogorov-Smirnov (KS) goodness-of-fit tests. Unfortunately straight forward application of both tests showed that the hypothesis of normally distributed time series observations can be rejected in virtually all cases. Yet, proper application of these and other similar goodness-of-fit tests requires that the data are a random sample of the true population with observations within the sample being independent. Such is not the case for the serially correlated swash time series. So even though the deviation results given by these tests are meaningful, the goodness-of-fit tests themselves are definitely non-optimal. However, this explanation is not meant to suggest that the swash time series observations are consistent with a linear, Gaussian process. In fact, it will be shown that significant discrepancies between the swash maxima observations and the CLH56 model often exist and that these discrepancies can be attributed to the nonlinearity of the swash process.

In order to develop an alternate measure of the degree of deviation from Gaussianity, third and fourth moment statistics were calculated for each of the swash time series. Figure II.8 shows a swash time series and associated histogram obtained using the video method. As seen in the figure, deviations from Gaussianity are reflected in the skewness (time series asymmetry about the horizontal axis), asymmetry (time series asymmetry about the vertical axis) and kurtosis (distribution peakedness) statistics. Using skewness, asymmetry and kurtosis as relative measures of the validity of the fundamental assumption, we will test model performance as a function of "linearity".

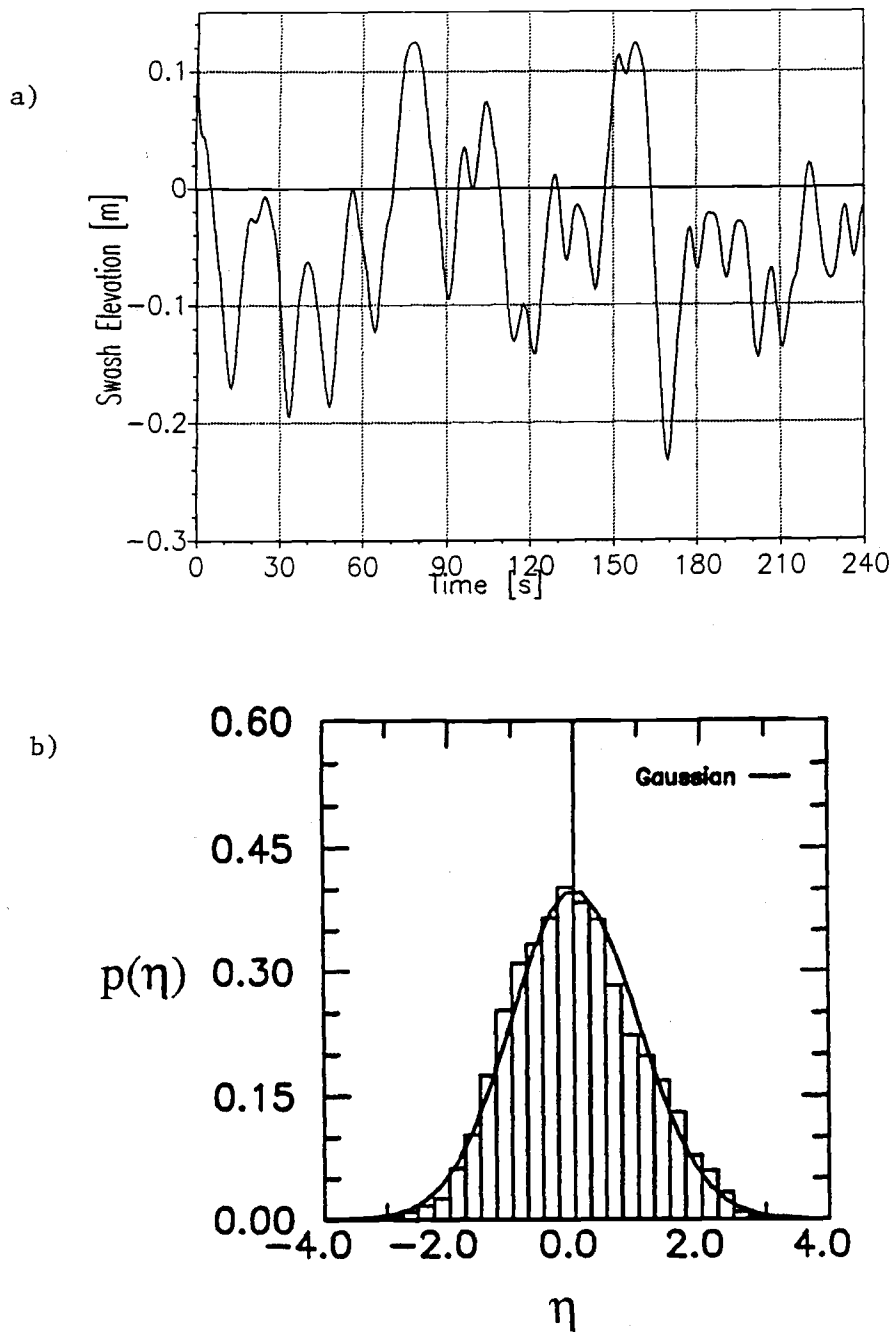

Figure II.8. a) Swash time series from the USWASH experiment and b) its corresponding normalized distribution. The standard normal distribution is given for comparison by the solid line. The time series skewness = 0.144, asymmetry 0.15 and kurtosis = 2.80.

Swash Maxima Distributions

Example probability density functions of swash maxima, ζ, and associated spectra from the DELILAH, LBIES and USWASH experiments are shown in Figure II.9. The theoretical probability density functions estimated using Equation (II.4) are also shown. For these examples, the agreement between the model and swash maxima observations is good. Note the trend in the observations that as ε increases the proportion of negative maxima increases, in agreement with the theory.

For the complete data set, spectral width values ranged between 0.76 to 0.96, the region of greatest sensitivity to ε (Figure II.3). In order to test the accuracy of the model to changes in ε, bulk measures of the distribution results were computed. Figure II.10 shows a plot of ε versus the average value of the swash maxima, denoted by $\bar{\zeta}$. Theoretical results are shown by the solid lines. The vertical bars represent the range of expected values determined using the simulations. By examining Figure II.10 we see that the mean maximum decreases significantly as ε increases, consistent with our expectations.

As a second bulk measure, observed spectral widths, ε_{obs}, were compared to best fit spectral width values, ε_{fit}, calculated from a numerical least squares fit of the observed maxima distribution to the model equation (4). The results are presented in Figure II.11. The approximately linear correlation between the two variables indicates that the observations and model expectations respond similarly to changes in ε. One possible explanation for the slight discrepancy between values is that ε_{obs} was calculated using Equation (5) as the integral from 0 to the filter cutoff frequency rather than infinity, giving slightly smaller estimates of ε_{obs} than would predicted directly from the maxima results.

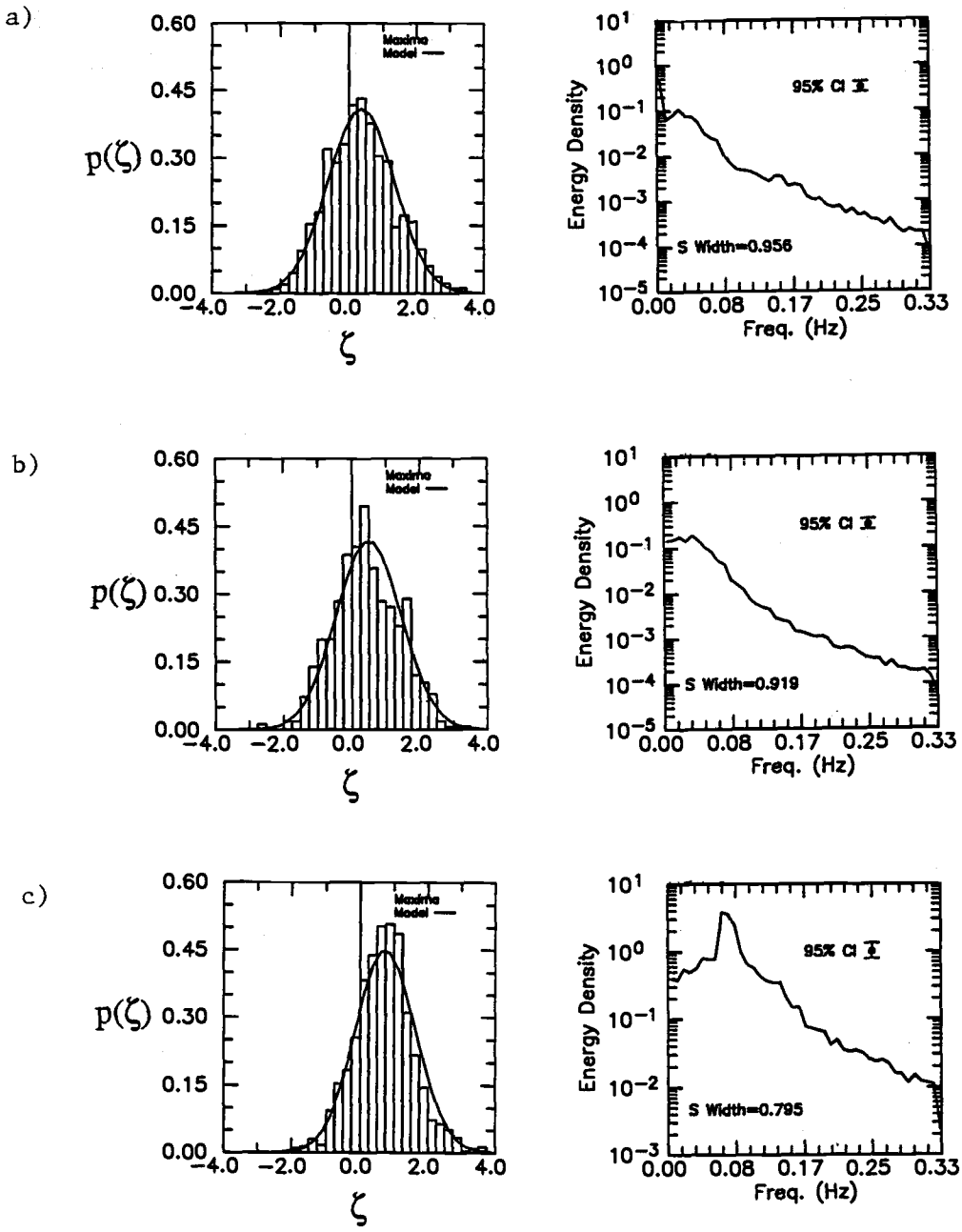

Figure II.9. Example maxima distributions and power spectra from the a) LBIES, b) USWASH, and c) DELILAH experiments.

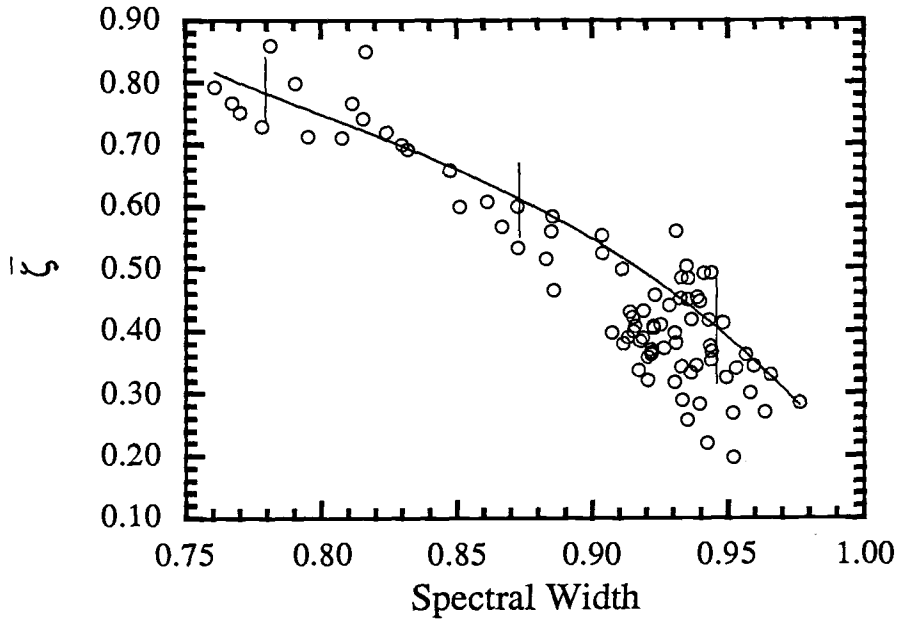

Figure II.10. Statistical measures of ζ as a function of spectral width. The statistics (circles) are taken from the ζ observations being normalized by $\sqrt{m_0}$. Theoretical results formulated using Equation (II.4) are shown as the solid line, with expected ranges indicated.

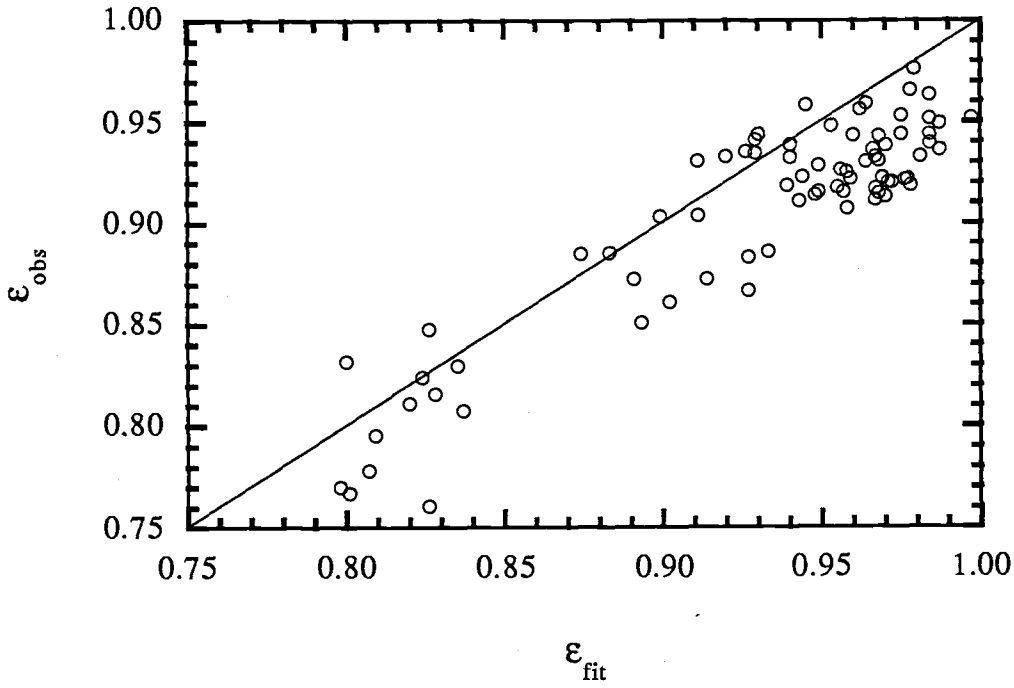

Figure II.11. Observed spectral width, ε_{obs}, plotted versus a calculated "least squares" spectral width value, ε_{fit}. The 45 degree line indicates the region of one to one correspondence.

In addition to the more integrated statistics describing the general form of the maxima distributions, probability of exceedence values describing the upper tail of the distribution were also calculated. Figure II.12 shows plots of ε versus the elevations at which 33, 10 and 2% of the normalized swash maxima were exceeded, denoted $\zeta_{33\%}$, $\zeta_{10\%}$, and $\zeta_{2\%}$ respectively. As in Figure II.10, the theoretical results and expected ranges are shown. For each statistic, the CLH56 theory predicts that as the spectral width increases, the area under the more positive tail decreases, thereby resulting in lower statistic values. In general, the results show this to be the case, especially for $\zeta_{33\%}$, although the scatter of the $\zeta_{10\%}$ and $\zeta_{2\%}$ results is considerable. However, as the expected ranges demonstrate, correlation between changes in spectral width and changes in the exceedence statistic decreases as the probability level, α, increases. So the increase in the scatter of the results with decreasing α is not surprising.

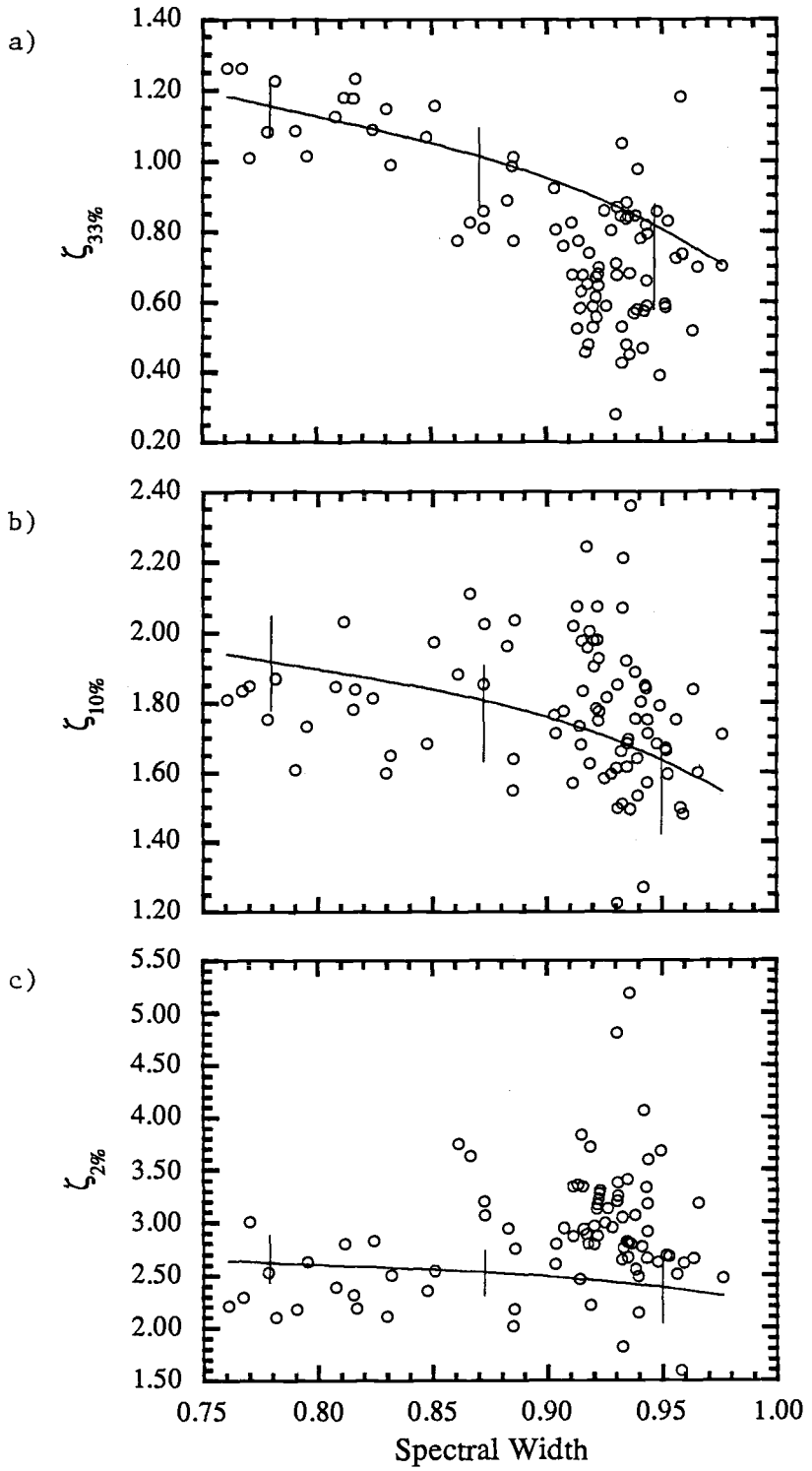

Figure II.12 a, b, c. Probability of exceedence levels as a function of spectral width. Theoretical results and expected ranges are shown as in Figure II.10.

Field Observation/Simulation Comparisons

The simulations can also be used to assess the significance of the field observations when compared to the model predictions. Taken as an ensemble of "synthetic observations", probability density functions for the various statistics were computed for comparison with the field data. This technique, known as the Monte Carlo method, was used to identify observed maxima distributions that can be approximated according to the CLH56 model. Although, as stated previously, goodness-of-fit statistical tests are not generally applicable to long time series due to serial correlation problems, the statistic values themselves provide a useful measure of the deviation of observations from theory. A hypothetical example is shown in Figure II.13, where the observed X^2 value describing the fit of maxima distribution to the pdf given by (4) is compared to the distributed ensemble of chi-square deviation values, χ^2, found using the simulations. Using a one-sided (upper tail) test, the region of acceptance of the null hypothesis that the maxima distribution can be approximated by the linear model is given by

$$X^2 \leq \chi^2_\alpha \qquad \text{(II.12)}$$

for a significance level, α. A sample value X^2 is greater than χ^2_α suggests that the null hypothesis should be rejected.

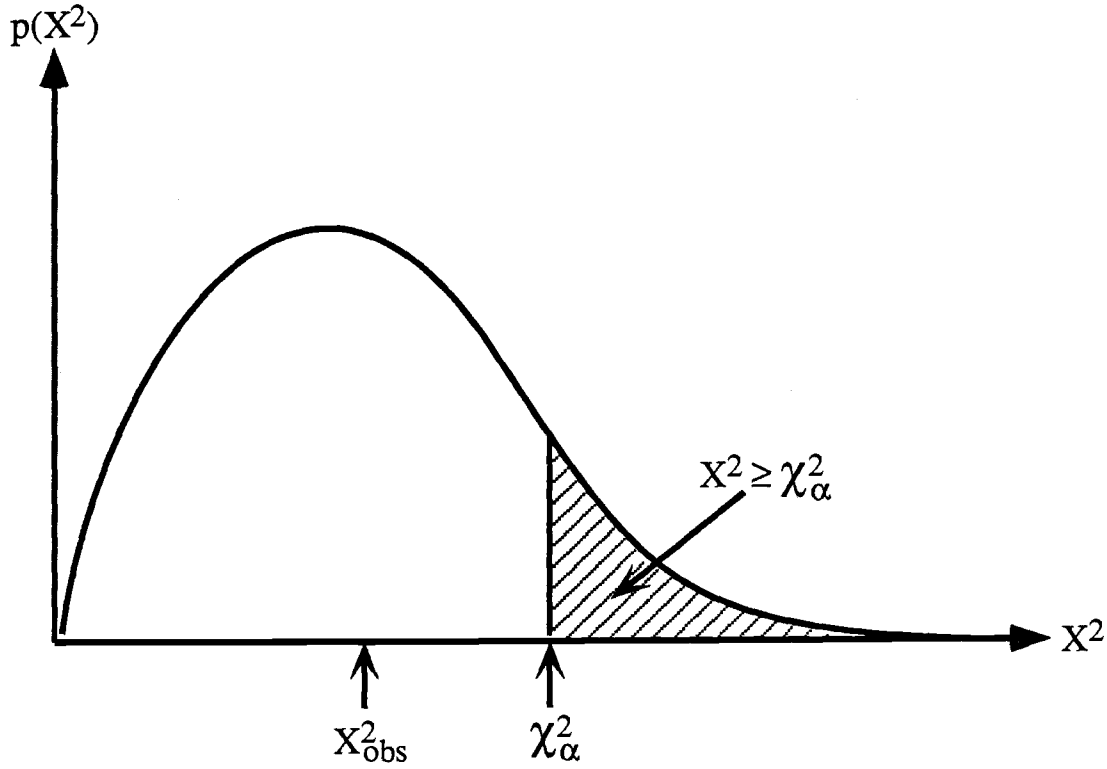

Figure II.13. Sketch of a significantly small observed X^2 deviation value. The shaded region corresponds to the area under the curve giving $X^2 \geq \chi^2_\alpha$.

Using this method, we observe that 88% of the runs have significantly large X^2 values, defined as being greater than 95% of the simulation X^2 values. The null hypothesis could not be rejected for the remaining 10 runs. Accordingly, the swash time series distributions that correspond with these 10 runs visually approximate a Gaussian distribution, consistent with the fundamental linear assumption.

Extreme Values

Table II.2 lists observed extreme probabilities from the 10 swash time series shown to have statistically similar maxima distributions to the linear simulations. Since the extreme value equations above are derived as an extension of the CLH56 model, extreme value predictions are not presented for those time series not well described by fundamental assumption. Predicted extreme values using the observed spectrum are shown for comparison. Also included are the probability values that would give predicted extremes equivalent to the observed extremes. Note that these probability levels are well contained within the distribution of possible extreme values, with an average α of 0.35. Additionally, we find that $\bar{\upsilon}$, the value for which the extreme value pdf becomes a maximum, generally underpredicts the observed extremes, serving only as rough approximation of the observations. Six of the ten time series have equivalent α values less than 0.2, with none of the observations exceeding the predicted extreme value, υ_α, for an α of 0.01. This suggests that perhaps $\upsilon_{\alpha=0.01}$ is more appropriate than $\bar{\upsilon}$, if conservative extreme value estimates are required for the design of shore protection structures.

Table II.2. Predicted and observed extreme value statistics for the 10 swash time series having maxima distributions statistically similar to the synthetic data.

Spectral Width, ε	Number of maxima, n	Observed Extreme Value, υ	Predicted Extreme Values				Equivalent α
			$\bar{\upsilon}$	$\upsilon_{\alpha=0.10}$	$\upsilon_{\alpha=0.05}$	$\upsilon_{\alpha=0.01}$	
0.80	761	4.07	3.59	4.16	4.32	4.68	0.15
0.81	631	3.53	3.53	4.11	4.28	4.63	0.90
0.81	803	3.65	3.60	4.17	4.33	4.68	0.76
0.85	767	4.63	3.57	4.14	4.31	4.66	0.01
0.90	1075	4.46	3.62	4.19	4.35	4.70	0.03
0.92	442	3.42	3.36	3.96	4.13	4.50	0.73
0.93	912	3.98	3.55	4.12	4.29	4.64	0.18
0.95	747	3.64	3.47	4.05	4.22	4.58	0.50
0.96	673	4.51	3.42	4.01	4.18	4.55	0.01
0.98	600	3.77	3.34	3.94	4.11	4.47	0.19

Nonlinearity results

The most likely explanation of discrepancies between the model and the data is that the fundamental assumption of a linear, Gaussian process is not strictly justified. Therefore, it is reasonable to expect that the magnitude of deviation should be reflected by the degree of nonlinearity suggested by various statistical measures. As seen in Figure II.14, a straightforward relationship exists between the chi-square deviation of the swash time series from the Gaussian distribution and the chi-square deviation of the maxima results from the model expectations. Simply put, the more non-Gaussian the swash time series, the farther the model expectations deviate from the maxima observations. A similar relationship exists between the maxima/model chi-square deviation and the skewness of the time series (Figure II.15). However, no particular correlation is apparent between the same deviation statistic and either the time series asymmetry or kurtosis values. Similarly, we found no consistent trends between the performance of the model and either the field site or the sampling method.

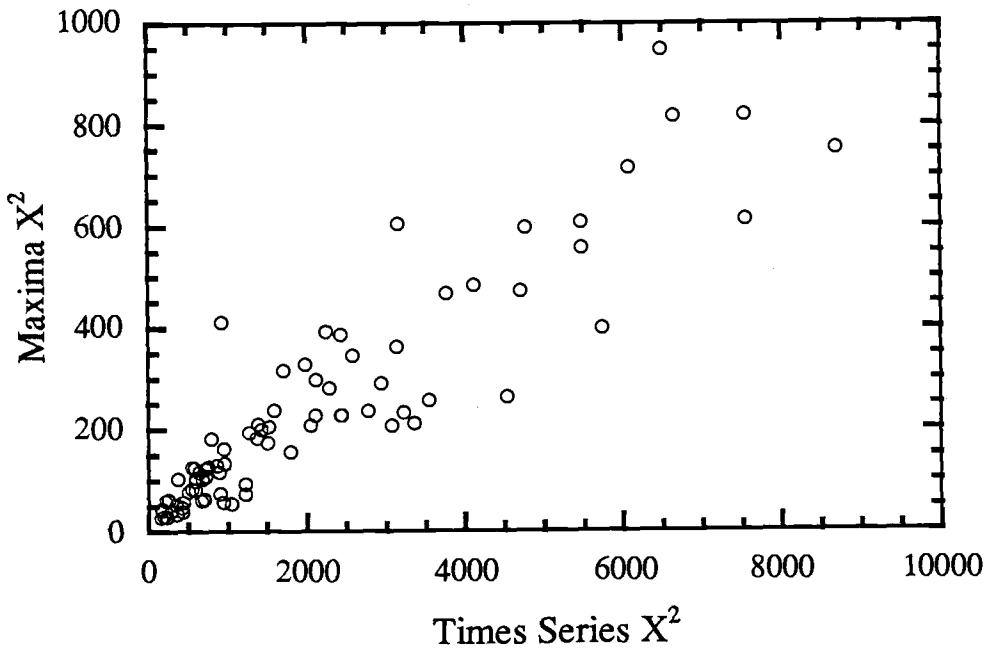

Figure II.14. X^2 deviation of the swash time series distribution from the Gaussian pdf plotted against X^2 deviation of the swash maxima distribution from the CLH56 model pdf.

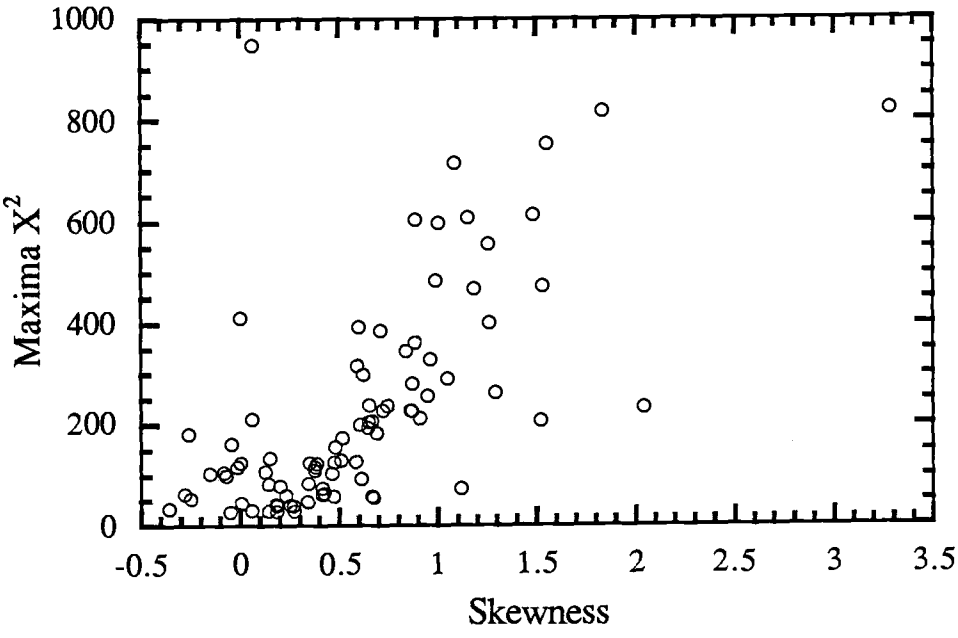

Figure II.15. X^2 deviation of the swash maxima distribution from the CLH56 model pdf as a function of time series skewness.

If we use skewness as a proxy for the degree of time series nonlinearity, we can examine the dependence of model performance on the fundamental assumption. The ratio of observed to predicted exceedence values for the $\zeta_{33\%}$, $\zeta_{10\%}$, and $\zeta_{2\%}$ statistics is plotted against time series skewness in Figure II.16. We observe that for low skewness values (suggestive of linearity), observed and predicted values are approximately equal. However, as skewness (nonlinearity) increases, the data systematically deviates from model predictions. Predicted values of $\zeta_{2\%}$ and $\zeta_{10\%}$ will underestimate observations if the swash time series has a positive skewness value of greater than 0.5. Similar skewnesses will give rise to overestimates of the $\zeta_{33\%}$ observations.

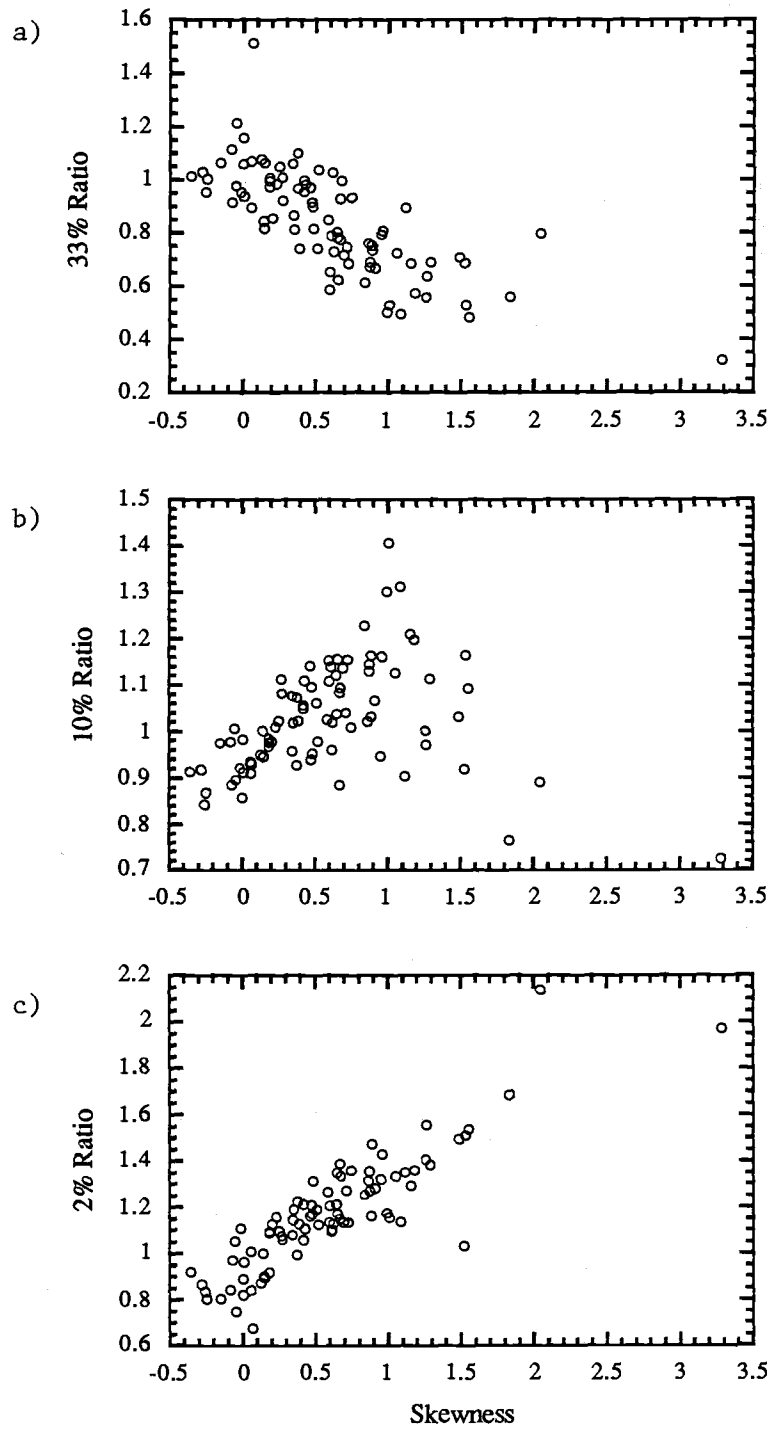

Figure II.16. Ratios of observed to predicted exceedence probabilities as a function of skewness. a) 33%, b) 10%, c) 2%.

Discussion

In the preceding sections, the application of a probabilistic model to runup field data has shown that swash maxima statistics and distributions are well approximated as a function of spectral width. Such an application has an advantage over existing runup maxima distribution models in that the required parameters have obvious physical implications. The probability distribution of the process maxima is known to the extent to which the spectral parameters ε and m_0 can be estimated. Equivalency need not be invoked. Nor are empirical coefficients required. All forms of the model predictions can be directly related to changes in the process spectrum.

We also find certain characteristics of the proposed model are similar to existing models. For example, although the equivalency based models (given by Equation II.2) are defined using zero crossing maxima, the zero-crossing definition of runup maxima for narrow-banded processes is equivalent to the local maxima definition. Therefore we can compare the maxima pdf predicted by the CLH56 model for $\varepsilon = 0$ with the pdf predicted for narrow-band spectra by the Battjes model. In both cases, the function is given by the Rayleigh distribution. For broader band spectra, laboratory researchers well aware of the Saville's results find irregular wave runup to be approximately Gaussian distributed, in agreement with our findings (Webber and Bullock, 1968). This model differs, however, from previous models in that the CLH56 theory allows for estimation of both positive and negative maxima.

Furthermore, a runup maxima model dependent upon the spectral width parameter is not without precedence. Van Oorschot and d'Angremond (1968) suggest that proper application of Hunt's equation (II.1) to irregular waves requires a variable proportionality factor, C, dependent upon spectral width. They observe that for a particular exceedence

probability, a wider spectrum produces a considerably higher runup maximum (defined using a zero-crossing method) than does a narrow spectrum. Both our field data and the CLH56 model indicate that as ε increases, the highest maximum in a sample of n maxima tends to decreases relative to $\sqrt{m_0}$. However, it can be shown that the highest maximum will increase relative to the r.m.s. height of the maxima (Cartwright and Longuet-Higgins, 1956). Although it is difficult to relate zero-crossing maxima findings to local maxima definitions, their observations support the idea that spectral width has direct implications on the form of the runup maxima probability distribution.

It is important to note that the parameters on which the model depends must be determined *a priori*. However, it is quite likely that calculation of these parameters from the data is not necessarily required. Accurate estimation of $\overline{\eta}$, ε, and m_0 may be possible given observations of a general form of the shoreline runup spectrum (Huntley et al., 1977; Guza and Thornton, 1982) and our present knowledge of setup dynamics (Bowen et al., 1968; Guza and Thornton, 1981; Holman and Sallenger, 1985).

Proper application of the CLH56 model to wave runup requires the assumption that runup is a linear, Gaussian process. We have observed that the validity of this assumption is restricted to particular instances. The results indicate that for those data where the assumption was not violated, the model gives meaningful results, even for extreme values. However, in numerous cases this assumption could not be justified, presumably due to nonlinearity, rendering the extreme predictions of the model inexact. There are several reasons to suspect the influence of nonlinearity in swash motions including composite sloped beach profiles, bed roughness, permeability, coherent bore-to-bore interactions and transformation of energy during wave shoaling. The specific influence of any or all of these possible causes is difficult to derive. Further research in this area is required to determine the validity of practical application of these observations.

Summary

Runup data from an extensive range of conditions were analyzed to determine if the probability density function of swash maxima could be described using a linear statistical model. This model makes no assumptions about the data other than the supposition of a Gaussian process and requires only two input parameters: the spectral width and root mean square values of the process of interest. Simulation results suggest that runup spectral forms are within the range of application of the theory. Field data taken under a variety of conditions indicate that various maxima statistics are well parameterized by ε and that the qualitative trends of the distribution response to changes in ε are appropriate. Few examples of statistically significant correspondence between the maxima pdf observations and the model were identified. However, extreme value prediction formulas derived as an extension to the statistical model were shown to be applicable in those cases where the fundamental assumption is justifiable. Time series skewness is suggested as the dominant parameter expressing the non-Gaussian characteristics of the swash motions.

Acknowledgements

The authors wish to thank the late Paul V. O'Neill for his insight as to the usefulness of the timestack technique and Christine Valentine for performing the majority of the video digitization. Tom Lippmann contributed valuable suggestions which were appreciated. We would like to give special thanks to Bob Guza for providing the runup wire data and helpful comments. The field programs were funded by the Office of Naval Research and by the U.S. Geological Survey. Data analysis was funded by the U.S. Geological Survey as part of the National Coastal Geology Program.

References

Aagard, T. and J. Holm, Digitization of wave runup using video records, *J. Coastal Res.*, 5, 547-551, 1989.

Ahrens, J. P., Irregular wave runup, *Coastal Structures '79*, Am. Soc. of Civil Eng., 998-1019, 1979.

Ahrens, J. P., Wave runup on idealized structures, *Coastal Structures '83*, Am. Soc. of Civil Eng., 925-938, 1983.

Battjes, J. A., Runup distributions of waves breaking on slopes, *J. Waterways, Harbors and Coastal Eng. Div.*, Am. Soc. of Civil Eng., 97, 91-114, 1971.

Bendat, J. S., and A. G. Piersol, *Random Data: Analysis and Measurement Procedures*, John Wiley, New York, 1986.

Birkemeier, W. A., K. K. Hathaway, J. M. Smith, C. F. Baron, and M.W. Leffler, DELILAH experiment: Investigator's summary report, Coastal Eng. Res. Cent., Field Res. Facil., U.S. Eng. Waterw. Exp. Sta., Vicksburg, Miss., 1991.

Bowen, A. J., D. L. Inman, and V. P. Simmons, Wave "set-down" and wave setup, *J. Geophys. Res.*, 73, 2569-2577, 1968.

Carrier, G. F. and H. P. Greenspan, Water waves of finite amplitude on a sloping beach, *J. Fluid Mech.*, 4, 97-109, 1958.

Cartwright, D. E. and M. S. Longuet-Higgins, The statistical distribution of the maxima of a random function, *Proc. R. Soc. London Ser. A*, 237, 212-232,1956.

Elgar S., R. T. Guza and R. J. Seymour, Groups of waves in shallow water, *J. Geophys. Res.*, 89, 3623-3634, 1984.

Elgar S., R. T. Guza and R. J. Seymour, Wave group statistics from numerical simulations of a random sea, *Applied Ocean Research*, 7, 93-96, 1985.

Guza, R. T. and E. B. Thornton, Wave setup on a natural beach, *J. Geophys. Res.*, 87, 4133-4137, 1981.

Guza, R. T. and E. B. Thornton, Local and shoaled comparisons of sea surface elevations, pressures, and velocities, *J. Geophys. Res.*, 85, 1524-1530,1980.

Guza, R. T. and E. B. Thornton, Swash oscillations on a natural beach, *J. Geophys. Res.*, 87, 483-491, 1982.

Holland, K. T. and R. A. Holman, Measuring runup on a natural beach II, *EOS, Trans, Am. Geophys. Union*, 72, 254, 1991.

Holman, R. A. and R. T. Guza, Measuring runup on a natural beach, *8th Coastal Engineering Conference Proceedings*, Am. Soc. of Civil Eng., 129-140, 1984.

Holman, R. A. and A. H. Sallenger, Setup and swash on a natural beach, *J. Geophys. Res.*, 90, 945-953, 1985.

Holman, R. A., Infragravity energy in the surf zone, *J. Geophys. Res.*, 87, 6442-6450, 1981.

Hunt, I.A., Design of seawalls and breakwaters, *Proc. Am. Soc. of Civil Eng.*, 85, 123-152, 1959.

Huntley, D. A., R. T. Guza and A. J. Bowen, A universal form for shoreline runup spectra?, *J. Geophys. Res.*, 82, 2577-2581, 1977.

LeMehaute, B., B. C. Y. Koh, and L-S. Hwang, A synthesis of wave runup, *J. Waterways and Harbors Division*, Am. Soc. of Civil Eng., 94, 77-92, 1968.

Lippmann, T. C. and R. A. Holman, Quantification of sand bar morphology: A video technique based on wave dissipation, *J Geophys. Res.*, 94, 995-1011, 1989

Miche, M., Le pouvoir reflechissant des ouvrage maritimes exposes a l'action de la houle, *Ann. Ponts. Chausses*, 121, 285-319, 1951.

Nielsen, P. and D. J. Hanslow, Wave runup distributions on natural beaches, *J. Coastal Res.*, 7, 1139-1152, 1991.

Ochi, M. K., On prediction of extreme values, *J. Ship Res.*, 17, 29-37, 1973.

Rice, S. O., The mathematical analysis of random noise, *Bell Sys. Tech. J.*, 23, 282-332, 1944; 24, 46-156, 1945.

Sallenger, A. H., S. Penland, S. J. Williams, and J. R. Suter, Louisiana barrier island erosion study, *Coastal Sediments '87*, Am. Soc. of Civil Eng., 1503-1516, 1987.

Saville, T., Jr., An approximation of the wave runup frequency distribution, *8th Coastal Engineering Conference Proceedings*, Am. Soc. of Civil Eng., 48-59, 1962.

Sawaragi, T. and K. Iwata, A nonlinear model of irregular wave runup height and period distributions on gentle slopes, *19th Coastal Engineering Conference Proceedings*, Am. Soc. of Civil Eng., 415-434, 1984.

Suhayda, J. N., Standing waves on beaches, *J. Geophys. Res.*, 79, 3065-3071, 1974.

Thornton, E. B. and R. T. Guza, Energy saturation and phase speeds measured on a natural beach, *J. Geophys. Res.*, 87, 9499-9508, 1982.

Van Oorschot, J. H. and K. d'Angremond, The effect of wave energy spectra on wave runup, *11th Coastal Engineering Conference Proceedings*, Am. Soc. of Civil Eng., 888-900, 1968.

Webber, N. B. and G.N. Bullock, A model study of the distribution of runup of wind-generated waves on sloping sea walls, *11th Coastal Engineering Conference Proceedings*, Am. Soc. of Civil Eng., 870-887, 1968.

CHAPTER THREE:

ESTIMATION OF OVERWASH BORE VELOCITIES USING VIDEO TECHNIQUES

Abstract

Overwash data were collected at a site on the Isles Dernieres, LA barrier island chain during Hurricane Gilbert in September 1988. A video technique was applied that allowed the quantification of overwash bore celerity vectors along several cross-shore transects. Maximum celerities were found to exceed 2 m/sec. The cross-beach velocity structure can be characterized generally as having a maximum celerity at the berm crest with a linear decrease in velocity across the washover flat. Using the celerity results, a simple model of cross-beach overwash sediment transport is discussed.

Introduction

Overwash is defined as a unidirectional flow of seawater, derived from wave action or storm surge, that overtops or breaches the highest berm or dune line of a barrier island. Pierce (1970) suggested that the overwash surge may contain sediment eroded by waves or could entrain sediment as it travels across the washover flat. As the flow subsides, the surge velocity decreases and sediment falls out of suspension, thereby increasing the elevation of the island landward of the maximum berm crest or dune line. In this manner, overwash can be an important depositional process in the landward migration of barrier islands. However, Ritchie and Penland, (1985) present evidence which indicates that overwash can be either accretional or erosional, depending on the amount of water transported landward across the barrier. Given the possibility of increasing erosion rates due to sea level rise, an ability to quantitatively describe overwash sediment transport dynamics is of great importance.

Cross-shore sediment transport rates have generally been accepted to be a function of velocity primarily to some power. However, few measurements of overwash velocities have been attempted, and the cross-beach structure of overwash velocities has yet to be accurately quantified. Fisher et al. (1974) measured a maximum overwash flow velocity of 2.4 m/sec with a sediment concentration of up to 50% sediment by weight at mid-depth in a 1 m deep channel on Assateague Island, MD. This single point measurement is useful as a reference, but certainly numerous measurements are required at a variety of positions across the beach to fully specify the velocity characteristics of the overwash flow. Our objective is to compute overwash celerity vectors along a number of cross-beach transects so that a simple model of overwash sediment transport can be developed.

Methods

Field Experiment

As part of the Louisiana Barrier Island Erosion Study (Sallenger et al., 1987), an experiment was designed to measure the physical parameters associated with overwash dynamics on Trinity Island, LA. This low-lying island (less than 1.6 m above MSL) is commonly subject to extensive overwash as part of the rapidly eroding (greater than 10 m/yr) Isles Dernieres barrier island chain off the central Gulf coast of Louisiana. The study area was chosen as being representative of the overwash sites in the Isles Dernieres in that it is topographically two dimensional with sparse vegetation and scattered dunes. During extreme storm conditions, overwash at this location has been observed to travel as a sheet flow rather than as channelized flow. The beach and washover flat are composed of a well-sorted, fine-grained sand with a mean grain size of 0.18 mm. Beach and nearshore profiles have been measured at the site approximately every three months and after large scale storms. Survey data are summarized in Dingler and Reiss (1988 and 1989).

A cross-beach instrument array and a video recording system were deployed between August 1987 and January 1990 to record the overwash bore propagation along a series of cross-beach transects through the center of a large washover flat. Figure III.1 is a map of the field site showing the ground coverage of the camera in relation to the berm crest and the cross-beach transect. Locations are defined using a left-hand coordinate system with the positive x direction directed landward and the positive y direction being alongshore to the east.

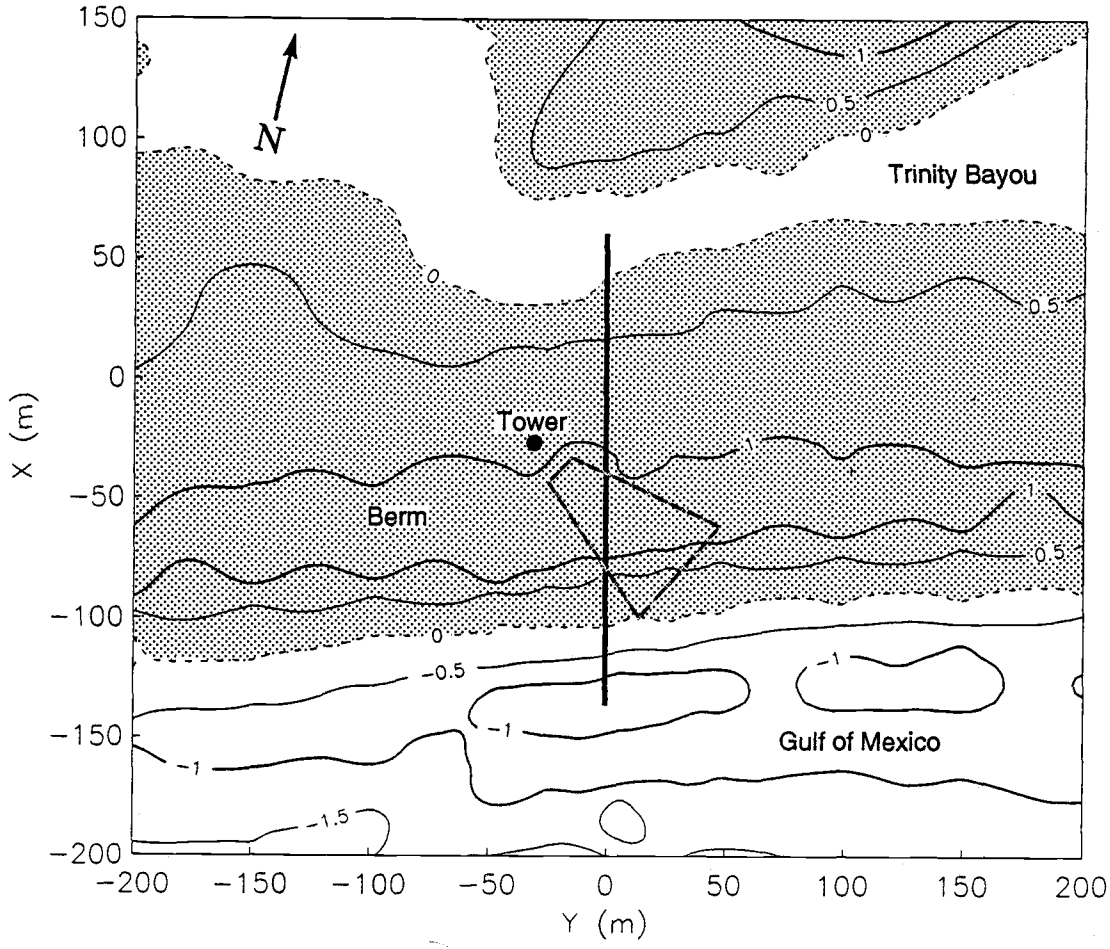

Figure III.1. Field map showing the study area topography and the cross-beach transect (signified by the solid line) in relation to the camera field of view (dashed).

To obtain background meteorological information, wind speed, wind direction and barometric pressure were measured on a 10-m tower constructed for the overwash experiment. Sea surface elevations were recorded by pressure gauges at two locations: a nearshore location 50 m from the shoreline in the Gulf of Mexico and a still water location in the bayou behind the island. Four subaerial, capacitance-type wave staffs were spaced along the cross-beach transect in line with the pressure gauge positions, starting seaward of the berm crest and continuing landward. The purpose of these sensors was to measure overwash flow depths during overwash "events" (here defined as the time interval of the storm during which the island is temporarily submerged by overwash flows). In addition, a video camera was mounted at the top of the tower to monitor the overwash bore propagation across the instrument transect. All instruments were hardwired to the tower location where the instrument signals were digitized and transmitted 32 km to a recording station on the mainland. The meteorological, pressure gauge and wave staff data were sampled at 2 Hz for approximately 34 minutes while the video data were recorded at 30 Hz with a total tape length of 2 hours.

The sampling scheme was automatically adjusted depending upon current oceanographic conditions. During non-overwash conditions portions of the instrument array were sampled 6 to 12 times daily on the hour. Overwash events were indicated by salt water flood switches located on posts situated near the berm crest that signaled the computer to increase the sampling of the entire instrument array to an hourly interval. During this "overwash mode" the video system was triggered to record synchronously with the instruments during daylight hours.

Since its emplacement, the instrument setup has successfully recorded more than 20 separate overwash events. The most significant event in terms of the magnitude of beach change occurred during Hurricane Gilbert, a catastrophic category 5 storm that made

landfall on the Yucatan peninsula, Mexico on September 14, 1988 and again in northeastern Mexico on September 16. This storm had a significant impact on the Isles Dernieres, with the berm crest being displaced 40 meters landward as documented by profiles taken before and after the storm (Figure III.2). The instrumentation performed flawlessly during the first two hours of significant overwash coinciding with this event; these are the data examined. Overwash depth measurements at the four wave staffs along the mainline transect were acquired synchronously with two 34-min. video recordings at 1700 and 1800 CST, September 14, 1988.

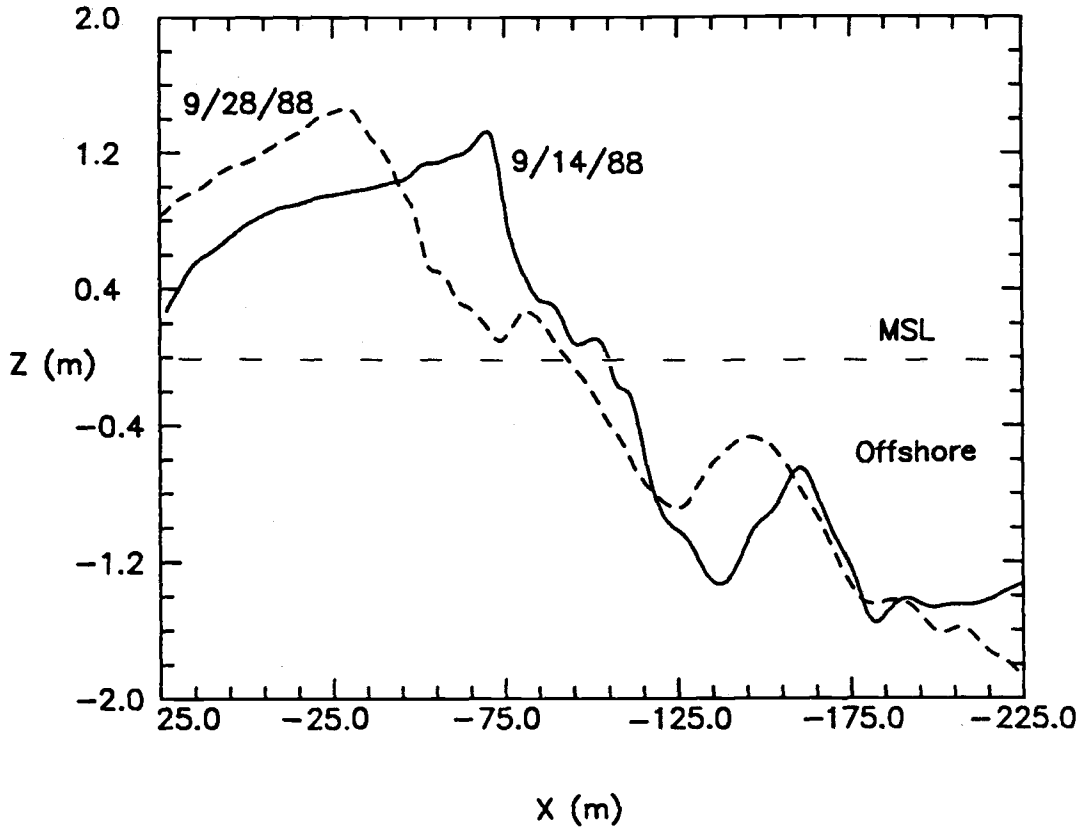

Figure III.2. Profile change along the instrument transect as a result of Hurricane Gilbert. The pre-storm profile is the solid line. The post-storm profile is dashed.

Data Analysis

In order to characterize the cross-beach velocity structure, Eulerian celerity vectors were determined at a variety of locations using a video technique based on our ability to quantify wave presence in terms of pixel intensities. Quite commonly, the edge of an overwash bore is identified in black and white video recordings by the presence of sea foam of a higher gray-scale intensity than that of the beach. Proven photogrammetric transformations described by Lippmann and Holman (1989) allow specific x,y,z ground coordinates within the field of view of a camera to be converted to x,y coordinates on a video image. Since overwash is a unidirectional flow, it is relatively easy to identify individual overwashes passing known ground locations by looking for a sharp gradient in the intensity time series sampled at corresponding image locations. To estimate an average overwash speed between two points with the distance between the points, Δl, being known, we simply compute the time lag, Δt, between the two time series using cross-correlation analyses. The apparent speed or celerity of the overwash in the direction of the diagonal connecting the two points, c_a, is then given by

$$c_a = \Delta l/\Delta t \tag{III.1}$$

where Δl is a constant and Δt is calculated. Computation of the true celerity vector, requires two orthogonal c_a estimates. To circumvent the problem of infinite apparent celerities ($\Delta t = 0$), the slowness, S, is defined as the reciprocal of the apparent celerity in each component. The magnitude, $|c|$, and direction, ϕ, of the overwash celerity vector is then given by:

$$|c| = \frac{1}{|S|} = \frac{1}{\sqrt{S_x^2 + S_y^2}} \tag{III.2}$$

$$\phi = \arctan\left(\frac{S_x}{S_y}\right) \tag{III.3}$$

To fully document the spatial homogeneity of the overwash bore propagation, celerity estimates at a variety of locations in both the longshore and the cross-shore were needed. Although traditional instrumentation, such as wave staffs and pressure gauges, can serve as indicators of overwash depths and velocities, accurate estimates of celerity vectors would necessitate a large number of sensors. The sampling problem is more easily overcome by using the above mentioned video technique. A 16m by 16m grid, incorporating 9 cross-beach transects, was centered within the camera's field of view. The most seaward point on each transect coincided with the berm crest, the highest point on the beach. Grid points were spaced every 2 meters giving a total of 64 locations at which celerity vectors would be determined. Time series of pixel intensity at each grid point were digitized at 10 Hz for the total 34-minute duration for each of the two runs using an Imaging Technology Inc. image processing system in a Sun 4/110 host computer. These time series were windowed to time intervals that coincided with the overwash bore propagation across the grid. Two-dimensional celerity vector maps were constructed for each data window using the cross-correlation celerity technique described above. Given a spatial resolution of ± 5 cm at the grid point farthest from the camera and a temporal resolution of ± 0.05 seconds, (with $l = 2$ m and $t = 1$ sec) the maximum error in the celerity magnitude measurements is approximately 15%.

Results

During the two 34-minute records, the berm was overtopped 48 times. Seventeen overwashes were selected for further analysis under the criterion that the entire grid area was covered. Although no periodicity was obvious to the eye, the average recurrence interval for these overwashes was approximately 240 seconds. The average cross-beach celerity at the berm crest was 2.0 m/sec with an average depth of 13 cm. The maximum cross-beach celerity of any single overwash was 2.9 m/sec and was located at the berm crest. Overwash propagation directions were not always shore normal and often exceed 30 degrees from landward. Figure III.3 shows several celerity vector maps that emphasize the variations of flow trajectories. Representative cross-beach celerity and depth profiles are shown in Figure III. 4. In general, we observe the maximum celerity and depth at the berm crest, decreasing with distance landward across the island.

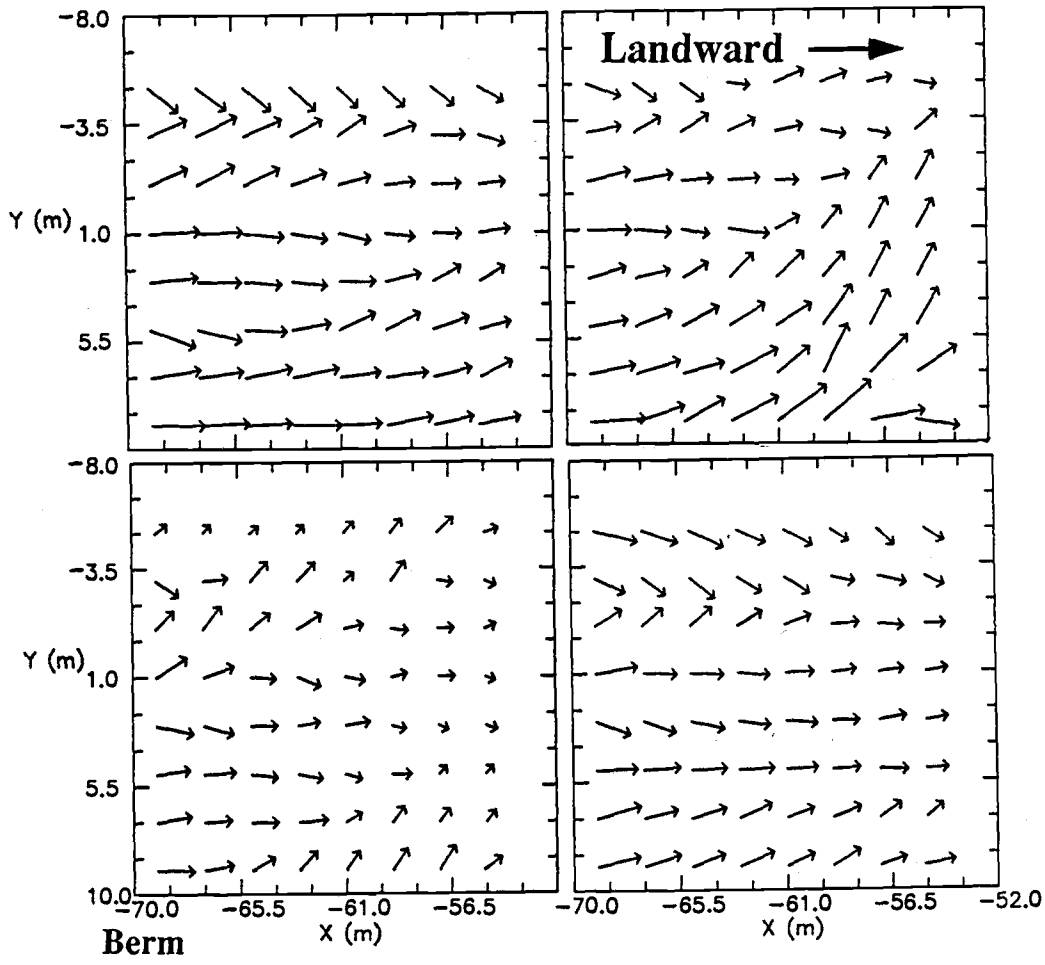

Figure III.3. Celerity vector maps showing contrasting overwash flow patterns. Cross-beach celerity gradients were calculated along transects that correspond to flow trajectories. ⟶ signifies a 1 m/sec flow.

In order to compute a characteristic celerity gradient along flow trajectories, 30 cross-beach velocity profiles were selected that had no significant longshore component. "Significant" was defined as a profile having at least one vector with a direction of more than 30 degrees from landward. Vector orientations of greater than 30 degrees are suggestive of flow intersecting the trajectory obliquely. Given the celerity magnitude error of 15%, it was difficult to justify anything other than a simple linear fit to the velocity profiles. Regression analyses were used to calculate the change in celerity with respect to distance for each profile. The result of these analyses was an average cross-beach celerity gradient of -0.05 m/sec/m with a standard deviation of 0.018 m/s/m. The negative gradient signifies deceleration. No consistent structure to the longshore celerity gradient was observed.

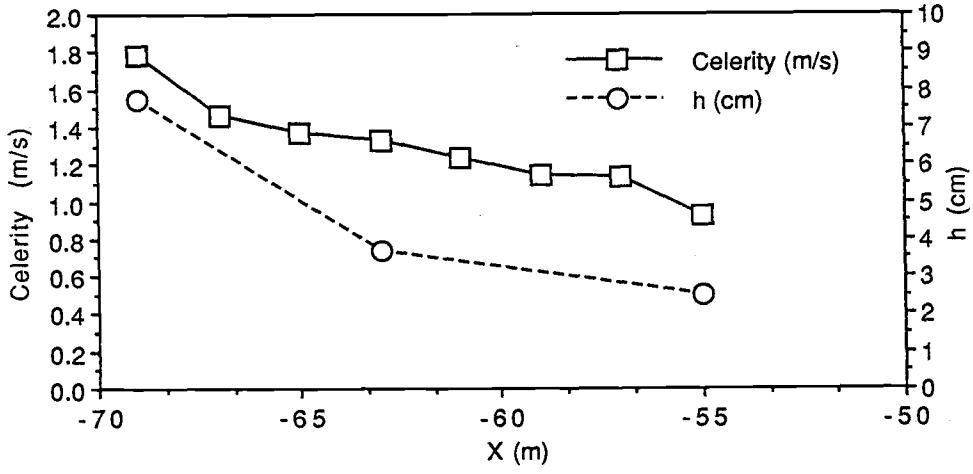

Figure III.4. Cross-beach celerity and depth profiles.

Discussion

Theoretical Expectations

It is useful to examine whether the overwash bore velocities satisfy expectations of velocity behavior for similar phenomena. One of the more obvious relationships to investigate is the relationship between velocity and flow depth. Linear wave theory predicts that the celerity of a wave travelling in shallow water is given by $c=\sqrt{gh}$, where h is the local water depth and g is the acceleration due to gravity. Clearly with a wave height of less than 0.25 m and a period on the order of 200 sec, the shallow water wave assumption is justified. Similarly, under finite amplitude wave conditions, a $\sqrt{gh}$ dependence can also be identified. Le Méhauté (1976) uses the method of characteristics to present the solution of the flow velocity at the leading edge of the bore as analogous to the breaking of a dam obtaining,

$$c = 2\sqrt{gh} \qquad \text{(III.4)}$$

where c = bore speed (m/sec) and h = the flow depth before collapse (m). This equation, developed for a horizontal, frictionless bottom, nevertheless indicates a general relationship between celerity and flow depth which should be similar to that of an overwash bore.

Observations

A comparison of the celerity magnitudes at three of the wave staff locations to the flow depths measured by the wave staffs at the same locations is shown in Figure III.5. The two curves showing the theoretical expectations of shallow water wave theory and bore theory are plotted. The symbols refer to the instrument location at which the data were measured. Celerity measurements at the most seaward wave staff were not calculated because the staff was situated outside the grid area.

The data can be grouped into two subsets; a set given by the measurements at the berm crest wavestaff, WS2, and a set including measurements at the two most landward staffs, WS3 and WS4. Interestingly, we see that the data from both sets lie above the shallow water wave celerity curve indicating that the overwash bore is travelling faster than linear theory would predict. Although there is a significant correlation between the celerities at the wave staff located at the berm crest and the flow depth at that location ($r^2 = 0.50$), the assumption that slope and flow depth are the only relevant parameters appears tenuous at best. However, the correlation between overwash celerity magnitude and flow depth at the two most landward locations appears to be more straightforward. Linear regression of the celerity and depth data at the two most landward wave staff locations identifies this relationship as $c = 2.6 \sqrt{gh}$ with a significant r^2 value of 0.77. This result indicates that overwash travels in a manner somewhat similar to what bore theory would predict, with flow depth being an important parameter governing overwash bore propagation. But the regression coefficient of 2.6 is greater than Le Méhauté's value of 2.0 suggesting that the influence of slope needs to be incorporated into the equation. We intend to pursue the effects of the pressure gradient, island slope, initial velocity, bed roughness and permeability in future studies.

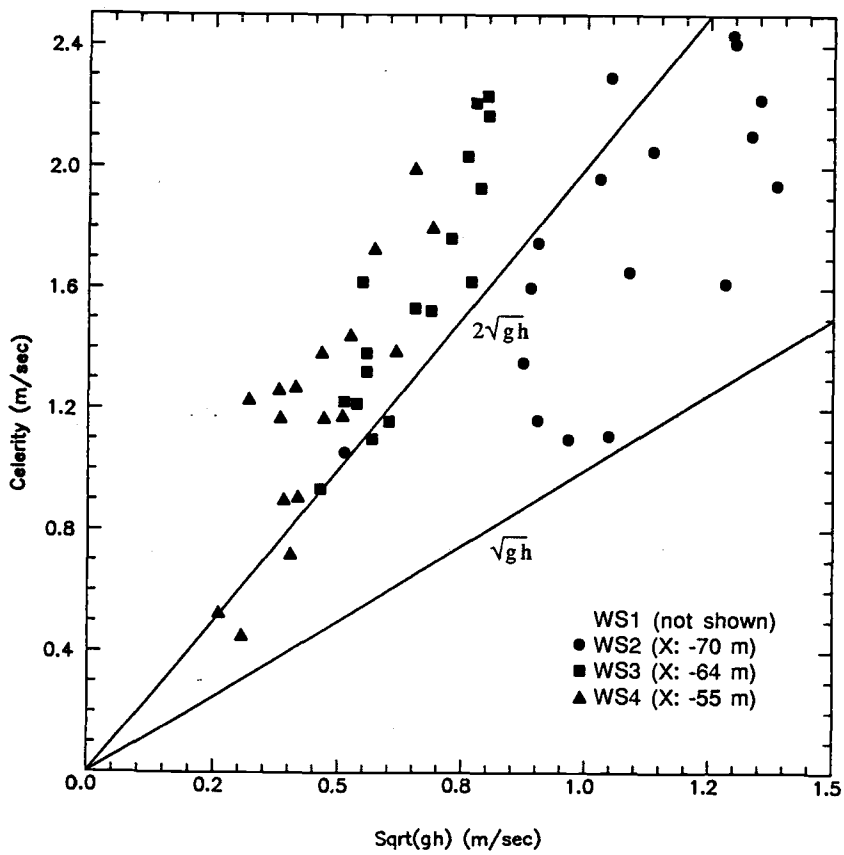

Figure III.5. Relationship between celerity magnitudes and flow depth at three wave staff locations. Curves represent theoretical expectations.

Implications for Sediment Transport

Numerous cross-shore sediment transport models have been developed showing the sediment transport to be proportional to the cross-shore fluid velocity, u, to some power. Bagnold's (1963) bedload sediment transport equation has a u^3 dependence and appears to be relevant to overwash-like flows. Therefore, taking the cross-shore volume transport, q_x, to be proportional to u^3 and neglecting the longshore sediment transport gradient, allows the time rate of change in beach elevation at a point, $\partial s/\partial t$, to be expressed using the sediment conservation equation as:

$$\frac{\partial s(x)}{\partial t} = -K \frac{\partial q_x(u)}{\partial x} \propto -3u^2 \frac{du}{dx} \qquad \text{(III.5)}$$

where K is the porosity correction factor needed to correct for void space and $\partial q_x/\partial x$ is the local divergence of cross-beach sediment transport.

Visual observations of the flow indicate that the fluid velocity is at least grossly approximated by the overwash bore celerity in the region behind the bore. Assuming the fluid velocity equals the bore velocity allows the substitution of the previously determined value of the average cross-beach celerity gradient, du/dx = -0.05 m/sec/m into equation 5. $\partial s/\partial t$ is therefore a positive quantity, indicating that the beach profile will aggrade landward of the berm crest. This result is in agreement with profile measurements (Figure III.2).

Summary

Results from a video technique to compute overwash bore celerity vectors have been presented. The technique relies on an ability to quantify bore propagation by comparing time series of pixel intensity at different locations. To our knowledge, this is the first time that such spatially extensive overwash velocity data have been quantified. Maximum celerities were found to exceed 2 m/s. Celerity orientations of greater than 30 degrees from landward were not uncommon.

The velocity profile along cross-beach trajectories was characterized as having a maximum at the berm crest and a linear decrease in velocity with distance across the overwash flat. Overwash bore velocities were shown to be a function of flow depth with magnitudes larger than simple bore theory would predict. Simple modelling of overwash sediment transport suggests that under the conditions sampled, overwash is a largely depositional process over the washover flat. The precise relationships between overwash velocities, slope, flow depths, bed roughness and surface permeability deserve further study.

Acknowledgements

We would like to thank Tom Lippmann and Paul O'Neill for providing valuable insight into our understanding of pixel dynamics. We would also like to thank the field crews of both the USGS and the LGS for their hard work in coaxing the instruments to function pseudo-continuously for over two years. Our appreciation goes to John Dingler and Tom Reiss for providing the survey data. This study was funded by the U.S. Geological Survey as part of the National Coastal Geology Program.

References

Bagnold, R.A., Mechanics of marine sedimentation. *The Sea*, Vol. 3, Wiley-Interscience, New York, NY, pp. 507-528, 1963.

Dingler, J.R. and T.E. Reiss, Louisiana Barrier Island Study: Isles Dernieres Beach Profiles August 1986 to September 1987, Open-File Report 88-7, U.S. Geological Survey, 27 pp., 1988.

Dingler, J.R. and T.E. Reiss, Louisiana Barrier Island Study: Isles Dernieres Beach Profiles September 1987 to September 1988, Open-File Report 89-89, U.S. Geological Survey, 23 pp., 1989.

Fisher, J.S., S.P. Leatherman, and F.C. Perry, Overwash processes on Assateague Island. *Proc. of the 14th Coastal Engineering Conference*, American Society of Civil Engineers, 1194-1212, 1974.

Le Méhauté, B., *An Introduction to Hydrodynamics and Water Waves*, Springer-Verlag, New York, NY, 315 pp., 1976.

Lippmann, T.C. and Holman, R.A., Quantification of sand bar morphology: a video technique based on wave dissipation, *J. Geophys. Res.*, 94: 995-1011, 1989.

Pierce, J.W., Tidal inlets and washover fans, *Journal of Geology*, 78: 230-234, 1970.

Ritchie, W. and Penland, S., Overwash process-response characteristics of landforms along the Caminada-Moreau coast, Louisiana, *Transgressive Depositional Environments of the Mississippi River Delta Plain, Guidebook Series No. 3*, Louisiana Geological Survey, Baton Rouge, LA, 141-174, 1985.

Sallenger, A.H., Jr., S. Penland, S.J. Williams, and J.R. Suter, Louisiana barrier island erosion study, *Coastal Sediments '87*, American Society of Civil Engineers, 1503-1516, 1987.

CHAPTER FOUR:
GENERAL CONCLUSIONS

Two aspects of beach response to overwash processes were investigated. The first involved an attempt to predict the distribution of maximum runup values on a natural beach. The obvious application of results concerning this aspect is to combine the form of the distribution with the magnitudes of contributions from regional forces (such as tides and storm surge) to develop a probability of overwash occurrence relationship for a particular location. The other aspect entailed measuring overwash bore celerities using video techniques. A first order parameterization of the cross-beach celerity gradient was extended to a simple model of overwash sediment transport.

Runup data from an extensive range of conditions were analyzed to determine if the probability density function of swash maxima could be described using a linear statistical model. This model makes no assumptions on the data other than the supposition of a Gaussian process and requires only two input parameters: the spectral width and root mean square values of the process of interest. Simulation results suggest that runup spectral forms are within the range of application of the theory. Field data results taken under a variety of conditions indicate that various maxima statistics are well parameterized by ε and that the qualitative trends of the distribution response to changes in ε are appropriate. Few examples of statistically significant correspondence between the maxima pdf observations and the model were identified. However, extreme value prediction formulas derived as an extension to the statistical model were shown to be applicable in those cases where the fundamental assumption is justifiable. Time series skewness was suggested as the dominant parameter expressing the non-Gaussian characteristics of the swash motions.

Results from a video technique to compute overwash bore celerity vectors have also been presented. The technique relies on an ability to quantify bore propagation by comparing time series of pixel intensity at different locations. To our knowledge, this is the first time that such spatially extensive overwash velocity data have been quantified. Maximum celerities were found to exceed 2 m/s. Celerity orientations of greater than 30 degrees from landward were not uncommon.

The velocity profile along cross-beach trajectories was characterized as having a maximum at the berm crest and a linear decrease in velocity with distance across the overwash flat. Overwash bore velocities were shown to be a function of flow depth with magnitudes larger than simple bore theory would predict. Simple modelling of overwash sediment transport suggests that under the conditions sampled, overwash is a largely depositional process over the washover flat.

The precise relationships between overwash velocities, slope, flow depths, bed roughness, surface permeability and sea level elevation forcing factors deserve further study. However, we have demonstrated that wave runup is an important process in determining how the beach responds to overwash. Furthermore, video-based measurement techniques have been shown to be satisfactory in terms of their extensive spatial coverages, accuracies and ease of deployment.

BIBLIOGRAPHY

Aagard, T. and J. Holm, Digitization of wave runup using video records, *J. Coastal Res.*, 5, 547-551, 1989.

Ahrens, J. P., Irregular wave runup, *Coastal Structures '79*, Am. Soc. of Civil Eng., 998-1019, 1979.

Ahrens, J. P., Wave runup on idealized structures, *Coastal Structures '83*, Am. Soc. of Civil Eng., 925-938, 1983.

Bagnold, R.A., Mechanics of marine sedimentation. *The Sea*, Vol. 3, Wiley-Interscience, New York, NY, pp. 507-528, 1963.

Battjes, J. A., Runup distributions of waves breaking on slopes, *J. Waterways, Harbors and Coastal Eng. Div.*, Am. Soc. of Civil Eng., 97, 91-114, 1971.

Bendat, J. S., and A. G. Piersol, *Random Data: Analysis and Measurement Procedures*, John Wiley, New York, 1986.

Birkemeier, W. A., K. K. Hathaway, J. M. Smith, C. F. Baron, and M.W. Leffler, DELILAH experiment: Investigator's summary report, Coastal Eng. Res. Cent., Field Res. Facil., U.S. Eng. Waterw. Exp. Sta., Vicksburg, Miss., 1991.

Bowen, A. J., D. L. Inman, and V. P. Simmons, Wave "set-down" and wave setup, *J. Geophys. Res.*, 73, 2569-2577, 1968.

Carrier, G. F. and H. P. Greenspan, Water waves of finite amplitude on a sloping beach, *J. Fluid Mech.*, 4, 97-109, 1958.

Cartwright, D. E. and M. S. Longuet-Higgins, The statistical distribution of the maxima of a random function, *Proc. R. Soc. London Ser. A*, 237, 212-232,1956.

Dingler, J.R. and T.E. Reiss, Louisiana Barrier Island Study: Isles Dernieres Beach Profiles August 1986 to September 1987, Open-File Report 88-7, U.S. Geological Survey, 27 pp., 1988.

Dingler, J.R. and T.E. Reiss, Louisiana Barrier Island Study: Isles Dernieres Beach Profiles September 1987 to September 1988, Open-File Report 89-89, U.S. Geological Survey, 23 pp., 1989.

Elgar S., R. T. Guza and R. J. Seymour, Groups of waves in shallow water, *J. Geophys. Res.*, 89, 3623-3634, 1984.

Elgar S., R. T. Guza and R. J. Seymour, Wave group statistics from numerical simulations of a random sea, *Applied Ocean Research*, 7, 93-96, 1985.

Fisher, J.S., S.P. Leatherman, and F.C. Perry, Overwash processes on Assateague Island. Proc. of the 14th Coastal Engineering Conference, American Society of Civil Engineers, 1194-1212, 1974.

Guza, R. T. and E. B. Thornton, Local and shoaled comparisons of sea surface elevations, pressures, and velocities, *J. Geophys. Res.*, 85, 1524-1530,1980.

Guza, R. T. and E. B. Thornton, Swash oscillations on a natural beach, *J. Geophys. Res.*, 87, 483-491, 1982.

Guza, R. T. and E. B. Thornton, Wave setup on a natural beach, *J. Geophys. Res.*, 87, 4133-4137, 1981.

Holland, K. T. and R. A. Holman, Measuring runup on a natural beach II, *EOS*, Trans, Am. Geophys. Union, 72, 254, 1991.

Holland, K. T., R. A. Holman, and A.H. Sallenger, Estimation of overwash bore velocities using video techniques, *Coastal Sediments '91*, Am. Soc. of Civil Eng., 489-497, 1991.

Holman, R. A. and A. H. Sallenger, Setup and swash on a natural beach, *J. Geophys. Res.*, 90, 945-953, 1985.

Holman, R. A. and R. T. Guza, Measuring runup on a natural beach, *8th Coastal Engineering Conference Proceedings*, Am. Soc. of Civil Eng., 129-140, 1984.

Holman, R. A., Infragravity energy in the surf zone, *J. Geophys. Res.*, 87, 6442-6450, 1981.

Hunt, I.A., Design of seawalls and breakwaters, *Proc. Am. Soc. of Civil Eng.*, 85, 123-152, 1959.

Huntley, D. A., R. T. Guza and A. J. Bowen, A universal form for shoreline runup spectra?, *J. Geophys. Res.*, 82, 2577-2581, 1977.

Le Méhauté, B., *An Introduction to Hydrodynamics and Water Waves*, Springer-Verlag, New York, NY, 315 pp., 1976.

LeMehaute, B., B. C. Y. Koh, and L-S. Hwang, A synthesis of wave runup, *J. Waterways and Harbors Division*, Am. Soc. of Civil Eng., 94, 77-92, 1968.

Lippmann, T. C. and R. A. Holman, Quantification of sand bar morphology: A video technique based on wave dissipation, *J. Geophys. Res.*, 94, 995-1011, 1989

Lippmann, T.C. and Holman, R.A., Quantification of sand bar morphology: a video technique based on wave dissipation, *J. Geophys. Res.*, 94: 995-1011, 1989.

Miche, M., Le pouvoir reflechissant des ouvrage maritimes exposes a l'action de la houle, *Ann. Ponts. Chausses*, 121, 285-319, 1951.

Nielsen, P. and D. J. Hanslow, Wave runup distributions on natural beaches, *J. Coastal Res.*, 7, 1139-1152, 1991.

Ochi, M. K., On prediction of extreme values, *J. Ship Res.*, 17, 29-37, 1973.

Pierce, J.W., Tidal inlets and washover fans, *J. Geology*, 78: 230-234, 1970.

Rice, S. O., The mathematical analysis of random noise, *Bell Sys. Tech. J.*, 23, 282-332, 1944; 24, 46-156, 1945.

Ritchie, W. and Penland, S., Overwash process-response characteristics of landforms along the Caminada-Moreau coast, Louisiana, Transgressive Depositional Environments of the Mississippi River Delta Plain, Guidebook Series No. 3, Louisiana Geological Survey, Baton Rouge, LA, 141-174, 1985.

Sallenger, A. H., S. Penland, S. J. Williams, and J. R. Suter, Louisiana barrier island erosion study, *Coastal Sediments '87*, Am. Soc. of Civil Eng., 1503-1516, 1987.

Saville, T., Jr., An approximation of the wave runup frequency distribution, *8th Coastal Engineering Conference Proceedings*, Am. Soc. of Civil Eng., 48-59, 1962.

Sawaragi, T. and K. Iwata, A nonlinear model of irregular wave runup height and period distributions on gentle slopes, *19th Coastal Engineering Conference Proceedings*, Am. Soc. of Civil Eng., 415-434, 1984.

Suhayda, J. N., Standing waves on beaches, *J. Geophys. Res.*, 79, 3065-3071, 1974.

Thornton, E. B. and R. T. Guza, Energy saturation and phase speeds measured on a natural beach, *J. Geophys. Res.*, 87, 9499-9508, 1982.

Van Oorschot, J. H. and K. d'Angremond, The effect of wave energy spectra on wave runup, *11th Coastal Engineering Conference Proceedings*, Am. Soc. of Civil Eng., 888-900, 1968.

Webber, N. B. and G.N. Bullock, A model study of the distribution of runup of wind-generated waves on sloping sea walls, *11th Coastal Engineering Conference Proceedings*, Am. Soc. of Civil Eng., 870-887, 1968.